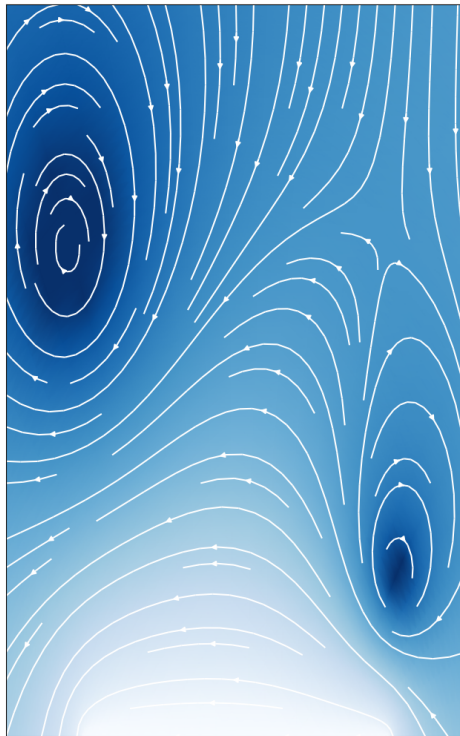


Calculating the magnetic field around a superconductor using complex conformal mappings

Tjipke Hofker - 4965558



BSC thesis
TU Delft
Applied Mathematics and Applied Physics
Delft, March 14, 2024

Supervisors: Dr. T. Van der Sar
Dr. W. Groenevelt
Ir. Roland Mulder
Committee: Dr Y. Blanter
Dr. J. Dubbeldam

Abstract

Superconductors expel magnetic fields, a phenomenon known as the Meissner effect. This effect makes it notoriously difficult to predict the magnetic field around a superconductor. One successful way of calculating these fields is through conformal mappings; coordinate transformations that preserve Maxwell's equations of magnetic fields in free space. These were first described by Norris[1] and later improved by Brandt[2][3]. In this bachelor thesis, conformal mappings are introduced and applied to 8 situations of magnetic field screening of an increasingly complex nature. We look at the screening of applied magnetic fields and of magnetic fields due to a bias current running through a wire itself. We later compare these results by experimental observations of the Van der Sar lab in Delft and measurements from other papers.

Contents

1. Introduction	1
2. Theory used in our applications	2
2.1 Superconductors	2
2.2 Complex conformal mappings	3
2.2.1 Schwarz–Christoffel	8
2.2.2 Joukowski mapping	9
3. Applications	10
3.1 Complete screening of an applied magnetic field over a thin sheet	10
3.2 Complete screening of a magnetic field magnetic due to bias current through a thin sheet	14
3.3 Complete screening of an applied magnetic field over a thick sheet	17
3.4 Complete screening of a magnetic field magnetic due to bias current through a thick sheet	17
3.5 Partial screening of applied magnetic field over a thin sheet	19
3.6 Partial screening of a magnetic field due to current through a thin sheet	23
3.7 Hysteresis of the magnetic field around a superconducting for AC currents or applied magnetic fields	24
3.8 Partial screening of an applied magnetic field and a magnetic field due current	26
4. Comparison with experimental results and discussion	32
5. Conclusion	35
A. Method of magneto-static images with circular boundary conditions	36
B. Current reconstruction from magnetic field	40
C. Proportionality of magnetic field to current distribution	42
D. Magnetic field around normal conducting sheet with applied current	44
E. code	44

1. Introduction

Superconductors are materials that exhibit zero electrical resistivity and an ability to expel magnetic fields, a phenomenon known as the Meissner effect. These properties give rise to highly non-trivial spatial current distributions within superconducting wires which play a central role in devices such as superconducting (Josephson) junctions[4], interference devices (SQUID magnetometers)[5], and qubits[6]. Ongoing research in the Van der Sar lab focuses on using nanoscale magnetic imaging based on nitrogen-vacancy spins in diamond to measure these current distributions with the overarching goal of understanding the more macroscopic current-voltage characteristics of these devices.

Mathematically, perfect expulsion of a magnetic field is impossible without creating singularities in our current distribution profile. In 1970, Norris[1] first calculated imperfect screening of the magnetic field due to a bias current through the wire. In his paper, he circumvented the singularities by limiting the maximum current density by a critical value J_c , where magnetic flux can penetrate the areas where the critical current density is reached. Brandt took this theory further and in 1993 he calculated the current distribution in a superconducting sheet when a perpendicular magnetic field is applied[2]. Later that year[3], Brandt combined his and Norris' theory to calculate incomplete shielding of a magnetic field, due to the combination of an applied field and a field due to current moving through the wire. In this paper, he also used Bean's theories[7][8] to calculate what happens with the current distribution when the magnetic field has an alternating strength, this is dubbed hysteresis.

These solutions make heavy use of conformal mappings, which is essentially a coordinate transformation that makes it much easier to calculate the current distributions. In this Bachelor's thesis, this formalism is explained and used to calculate the spatial current distributions in superconductors.

In section 2, we start by introducing the theory required for our calculations. This consists of introductions for superconductors and conformal mappings. In particular, the Schwarz-Christoffel and Joukowski transformations are described in detail for they are heavily used in our applications. Then in section 3 we will apply this theory to calculating magnetic fields around superconductors. First, perfect screening is shown for an applied magnetic field and a magnetic field due to current running through the sheet itself. These calculations will be done for an infinitely thin sheet and a slab where we cannot neglect its thickness. After, we will describe Norris' and Brandt's calculations for partial screening, hysteresis, and a when subjected to a field combined of an applied magnetic field and a field due to a bias current. In section 4 we will compare these equations with results from literature and the Van der Sar lab, and discuss the shortcomings of our approximations. We will also be referring to more recent papers by Cun Xue [9] and Brandt[10]. Our findings are summarized in section 5.

This thesis is written for the course TN2983 Bachelor Thesis, as part of the double BSc Applied Physics and Applied Mathematics at the Delft University of Technology, to be defended publicly on Monday, February 26, 2024, at 14:15 in the 'Van Katwijkzaal' (building 36 Electrical Engineering, Mathematics and Computer Sciences HB 08.150).

2. Theory used in our applications

In this section, we will explain in detail the theory used to analyze the current distribution in a superconductor. We will first introduce a small amount of theory on superconductors. This is explained in section 2.1, and is only meant to introduce the problem we will face and the boundary conditions we will introduce when setting up our boundary value problems.

Next, we will look at the behavior of conformal mappings and why they are useful for solving our problems in section 2.2. In this section, we will also go into detail on the Schwarz-Christoffel transformations, which are used to create a rich family of conformal mappings, and we will look at the Joukowski mapping, which can be used to rewrite boundary conditions from a straight line to a semi-circle. Both will be used heavily in section 3, where we will look at applications of the theory.

2.1. Superconductors

Since its prediction in 1913, superconductors have been the source of many important applications, like superconducting (Josephson) junctions[4], interference devices (SQUID magnetometers)[5], and qubits[6]. Some materials can reach a superconducting state when cooled down, and these are called superconductors. The temperature below which a material reaches its superconducting state will be denoted by T_c (its critical temperature). In simplest terms, a superconductor is called a 'super' conductor because there is zero dissipation for DC (Direct Currents) moving through. Another peculiar effect superconductors show is the Meissner effect; which, in simple terms, expels a magnetic field applied to a superconductor to be screened by currents running through the material itself. This is schematically shown in figure 1. As a notable result, a magnet can hover above a superconductor, as shown in figure 2.

This effect will give us our first boundary condition for our calculations around superconductors: the magnetic field is parallel to the superconducting surface if perfect shielding is assumed. Soon we will see that this effect is not always possible, and there will always be a slight magnetic flux penetration at every corner. This penetration is due to mathematical symmetry and is distinct from the London penetration depth, which we will be neglecting in our approximations.

For any calculations concerning magnetic fields and currents, we will need the Maxwell equations. They explain how the magnetic field disperses in free space. The equations we will be using are Amperes circuit law, and Gauss' law for magnetism in a stationary situation:

$$\vec{\nabla} \cdot \vec{H} = 0, \tag{1}$$

$$\vec{\nabla} \times \vec{H} = \vec{J}. \tag{2}$$

Here H is the magnetic field, and J is the current density. These equations will later be the conditions for our magnetic field in space free of charge and current. These will be combined after we find out about the magnetic scalar potential in the next section.

A magnetic scalar potential can be defined as $\phi = \nabla H$. Which can be combined with the previous equations to form a combined condition for the magnetic field:

$$\Delta\phi = \nabla^2\phi = 0. \tag{3}$$

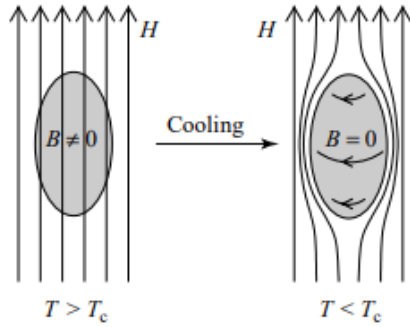


Figure 1: Schematic figure of Meissner effect when cooling down a superconductor to below its critical temperature T_c . The magnetic field lines bend around the superconductor due to the current moving inside the SC. From *K. Fosshem and A. Sudbø's Superconductivity*[11]

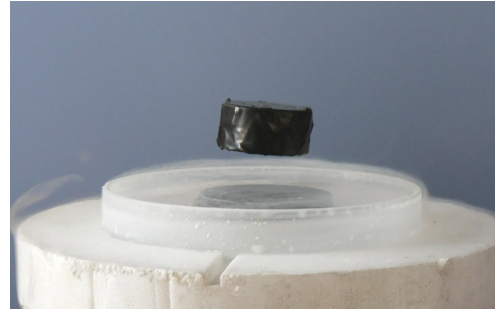


Figure 2: A combination of the Meissner effect and vortex pinning causes a superconductor to levitate above a magnet. From Britannica encyclopedia [12].

This will be our condition for the magnetic field outside of our sheet.

2.2. Complex conformal mappings

In this section, we assume experience with complex variables and functions. We will shortly discuss differentiability, and find the Cauchy-Riemann conditions. Then we will state two theorems that give motivation for mapping magnetic fields with conformal mappings. Then we will extend our scalar potential to the complex potential, and lastly, we will analyze two kinds of conformal mappings heavily used in the latter sections.

We start with a complex number $z = x + iy$, and a domain \mathcal{S} (always open and connected). If each point $z \in \mathcal{S}$ has a corresponding point $w = f(z)$, we can consider f as a mapping or transformation of the z -plane to the w -plane. We write f as a sum of a real and imaginary function $f(z) = u(x, y) + iv(x, y)$, and therefore we also write $w = u + iv$. f is differentiable at $z_0 \in \mathcal{S}$ if the limit

$$\lim_{\Delta z \rightarrow 0} \left(\frac{f(z_0 + \Delta z) - f(z_0)}{\Delta z} \right). \quad (4)$$

exist. Note that Δz is also a complex number; thus, the limit should hold for all directions. This limit is the derivative of f at z_0 , and is denoted as $f'(z_0)$ or $\frac{df}{dz}|_{z_0}$.

A function is analytic at a point or in a region if it is differentiable at a neighborhood around that point or all points in that region respectively. To obtain the Cauchy-Riemann equations we first look at this limit with $\Delta z_1 = \Delta x$, and $\Delta z_2 = i\Delta y$:

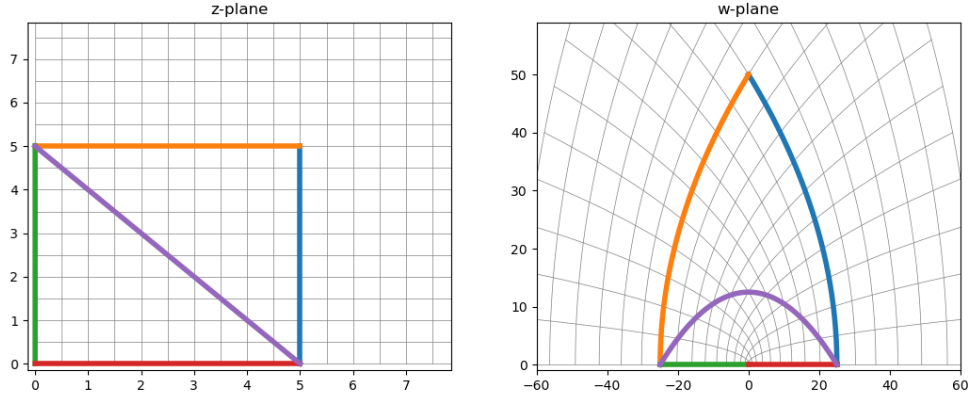


Figure 3: The mapping $w(z) = z^2$ looks conformal on the points $z \in \{5, 5 + 5i, 5i\}$, but not on $z = 0$. $w(z)$ will later be shown to be conformal on $\mathbb{C} \setminus \{0\}$

$$\begin{aligned}
 f'(z) &= \lim_{\Delta x \rightarrow 0} \left(\frac{u(x + \Delta x, y) + iv(x + \Delta x, y) - u(x, y) - iv(x, y)}{\Delta x} \right), \\
 &= u_x + iv_x, \\
 &= \lim_{\Delta y \rightarrow 0} \left(\frac{u(x, y + \Delta y) + iv(x, y + \Delta y) - u(x, y) - iv(x, y)}{i\Delta y} \right), \\
 &= -iu_y + v_y.
 \end{aligned}$$

This directly implies the Cauchy-Riemann equations:

$$\begin{aligned}
 u_x &= v_y, \\
 v_x &= -u_y.
 \end{aligned} \tag{5}$$

Note that this is a necessary condition for all analytic functions f . A quick look can therefore show that $f(z) = \bar{z} = x - iy$ is not analytic anywhere, since $u_x = 1 \neq -1 = v_y$.

We state two fundamental theorems. These will allow us to find solutions to magneto-static boundary condition problems and map them with a complex function $f(z)$ to a new plane where the solutions will stay valid.

Theorem 2.1. *All complex analytic functions $f(z)$ on a domain \mathcal{S} that are one-to-one on their co-domain \mathcal{S}' are conformal, at all points where $f'(z) \neq 0$.*

This problem is proven in many textbooks about conformal mappings or complex analysis[13]. Now for our second theorem:

Theorem 2.2. *Consider a twice differentiable scalar potential $\phi(z)$, with $z = x + yi$ on the domain \mathcal{S} , and an analytic complex function $w = f(z) \forall z \in \mathcal{S}$ mapping the z -plane to the w -plane. If $f'(z) \neq 0$ and $\Delta_{xy}\phi(z) = 0$ then $\Delta_{uv}\phi(w) = 0$ as well.*

Proof. We can apply the chain rule for partial derivatives to the first derivative of ϕ to obtain:

$$\frac{\partial \phi}{\partial x} = \frac{\partial u}{\partial x} \frac{\partial \phi}{\partial u} + \frac{\partial v}{\partial x} \frac{\partial \phi}{\partial v}. \quad (6)$$

Using the product rule we get the second derivative:

$$\begin{aligned} \frac{\partial^2 \phi}{\partial x^2} &= \frac{\partial}{\partial x} \left(\frac{\partial u}{\partial x} \frac{\partial \phi}{\partial u} + \frac{\partial v}{\partial x} \frac{\partial \phi}{\partial v} \right), \\ &= \frac{\partial^2 u}{\partial x^2} \frac{\partial \phi}{\partial u} + \frac{\partial u}{\partial x} \frac{\partial^2 \phi}{\partial u \partial x} + \frac{\partial^2 v}{\partial x^2} \frac{\partial \phi}{\partial v} + \frac{\partial v}{\partial x} \frac{\partial^2 \phi}{\partial v \partial x}. \end{aligned}$$

Now we apply equation 6 again:

$$\begin{aligned} \frac{\partial^2 \phi}{\partial x^2} &= \frac{\partial^2 u}{\partial x^2} \frac{\partial \phi}{\partial u} + \frac{\partial u}{\partial x} \frac{\partial}{\partial u} \left(\frac{\partial u}{\partial x} \frac{\partial \phi}{\partial u} + \frac{\partial v}{\partial x} \frac{\partial \phi}{\partial v} \right), \\ &\quad + \frac{\partial^2 v}{\partial x^2} \frac{\partial \phi}{\partial v} + \frac{\partial v}{\partial x} \frac{\partial}{\partial v} \left(\frac{\partial u}{\partial x} \frac{\partial \phi}{\partial u} + \frac{\partial v}{\partial x} \frac{\partial \phi}{\partial v} \right). \end{aligned}$$

Before we break open the brackets using the product rule again, we note that:

$$\begin{aligned} \frac{\partial^2 u}{\partial x \partial u} &= \frac{\partial}{\partial x} \frac{\partial u}{\partial u} = 0, \\ \frac{\partial^2 u}{\partial v \partial x} &= \frac{\partial^2 v}{\partial v \partial y} = \frac{\partial}{\partial y} \frac{\partial v}{\partial v} = 0. \end{aligned}$$

Where we used the Cauchy-Riemann equation 5 in the second line. This leads to:

$$\begin{aligned} \frac{\partial^2 \phi}{\partial x^2} &= \frac{\partial^2 u}{\partial x^2} \frac{\partial \phi}{\partial u} + \frac{\partial u}{\partial x} \left(\frac{\partial u}{\partial x} \frac{\partial^2 \phi}{\partial u^2} + \frac{\partial v}{\partial x} \frac{\partial^2 \phi}{\partial u \partial v} \right) \\ &\quad + \frac{\partial^2 v}{\partial x^2} \frac{\partial \phi}{\partial v} + \frac{\partial v}{\partial x} \left(\frac{\partial u}{\partial x} \frac{\partial^2 \phi}{\partial v \partial u} + \frac{\partial v}{\partial x} \frac{\partial^2 \phi}{\partial v^2} \right). \end{aligned}$$

The same approach to $\frac{\partial^2 \phi}{\partial y^2}$ would lead to

$$\begin{aligned} \frac{\partial^2 \phi}{\partial y^2} &= \frac{\partial^2 u}{\partial y^2} \frac{\partial \phi}{\partial u} + \frac{\partial u}{\partial y} \left(\frac{\partial u}{\partial y} \frac{\partial^2 \phi}{\partial u^2} + \frac{\partial v}{\partial y} \frac{\partial^2 \phi}{\partial u \partial v} \right), \\ &\quad + \frac{\partial^2 v}{\partial y^2} \frac{\partial \phi}{\partial v} + \frac{\partial v}{\partial y} \left(\frac{\partial u}{\partial y} \frac{\partial^2 \phi}{\partial v \partial u} + \frac{\partial v}{\partial y} \frac{\partial^2 \phi}{\partial v^2} \right). \end{aligned}$$

And thus the Laplace operator becomes:

$$\begin{aligned}
\Delta_{x,y}\phi &= \frac{\partial^2\phi}{\partial x^2} + \frac{\partial^2\phi}{\partial y^2} \\
&= \frac{\partial^2 u}{\partial x^2} \frac{\partial\phi}{\partial u} + \frac{\partial u}{\partial x} \left(\frac{\partial u}{\partial x} \frac{\partial^2\phi}{\partial u^2} + \frac{\partial v}{\partial x} \frac{\partial^2\phi}{\partial u\partial v} \right) + \frac{\partial^2 v}{\partial x^2} \frac{\partial\phi}{\partial v} + \frac{\partial v}{\partial x} \left(\frac{\partial u}{\partial x} \frac{\partial^2\phi}{\partial v\partial u} + \frac{\partial v}{\partial x} \frac{\partial^2\phi}{\partial v^2} \right) \\
&\quad + \frac{\partial^2 u}{\partial y^2} \frac{\partial\phi}{\partial u} + \frac{\partial u}{\partial y} \left(\frac{\partial u}{\partial y} \frac{\partial^2\phi}{\partial u^2} + \frac{\partial v}{\partial y} \frac{\partial^2\phi}{\partial u\partial v} \right) + \frac{\partial^2 v}{\partial y^2} \frac{\partial\phi}{\partial v} + \frac{\partial v}{\partial y} \left(\frac{\partial u}{\partial y} \frac{\partial^2\phi}{\partial v\partial u} + \frac{\partial v}{\partial y} \frac{\partial^2\phi}{\partial v^2} \right) \\
&= \left(\frac{\partial u}{\partial x} \right)^2 \frac{\partial^2\phi}{\partial u^2} + \left(\frac{\partial u}{\partial x} \right)^2 \frac{\partial^2\phi}{\partial v^2} + \left(\frac{\partial u}{\partial y} \right)^2 \frac{\partial^2\phi}{\partial u^2} + \left(\frac{\partial u}{\partial y} \right)^2 \frac{\partial^2\phi}{\partial v^2} \\
&= (u_x^2 + v_x^2) \left(\frac{\partial^2\phi}{\partial u^2} + \frac{\partial^2\phi}{\partial v^2} \right) \\
&= |f'(z)|^2 \Delta_{u,v}\phi.
\end{aligned} \tag{7}$$

Where all similarly underlined elements in the second line can be shown to cancel out using the Cauchy-Riemann conditions (equation 5). This equation directly implies that if the Laplace equations in the z -plane equal zero, then so does the Laplace equation in the w -plane, if f' is non-zero. This result finishes the proof. \square

These two theorems lead to a method of solving unique boundary conditions for magneto-statics; if a problem is hard to solve in a certain w plane, but we know a mapping of a z plane where the conditions are easy to satisfy, we can just use that solution and map it to our w plane, and have it solved.

The last useful tool we shall look at and use is the extension of our magnetic potential ϕ to a complex potential \mathcal{A}

Definition 2.3 (complex potential). *Consider a twice differentiable potential function $\phi(x, y)$ on \mathcal{S} . We now define the **complex potential** as the analytic complex function extension $\mathcal{A}(x, y) = \phi(x, y) + i\theta(x, y)$. Here θ is called the streamline function.*

The function $\theta(x, y)$ is named **stream function** from fluid mechanics and is unique up to a constant (as seen by Cauchy Riemann). In our applications, we still primarily consider the differential of the scalar potential as our field vector, thus $\nabla\phi = H(x, y)$. By extending our potential in the complex plane the magnetic field becomes (using Cauchy-Riemann once) $\overline{\mathcal{A}'} = \phi_x - i\theta_x = \phi_x + i\phi_y = H$, giving us an easy way to calculate H .

$$\overline{H}(z) = \frac{d\mathcal{A}}{dz} \tag{8}$$

Also, $\nabla\theta$ is not entirely useless since it gives us the directions of the equipotential lines around each point. This can be calculated from \mathcal{A} using Cauchy-Riemann: $\mathcal{A}' = -i\phi_y + \theta_y = -i\theta_x + \theta_y = \frac{1}{i}(\theta_x - i\theta_y) = \frac{1}{i}\overline{\nabla\theta}$, thus $\nabla\theta = i\overline{\mathcal{A}'}$ which is the orthogonal line to H and therefor it shows the direction of the equipotential lines in \mathcal{S} . In figure 4 we show the real and imaginary part of the complex potential $\mathcal{A} = z^2$, and depict the direction of the field and equipotential lines.

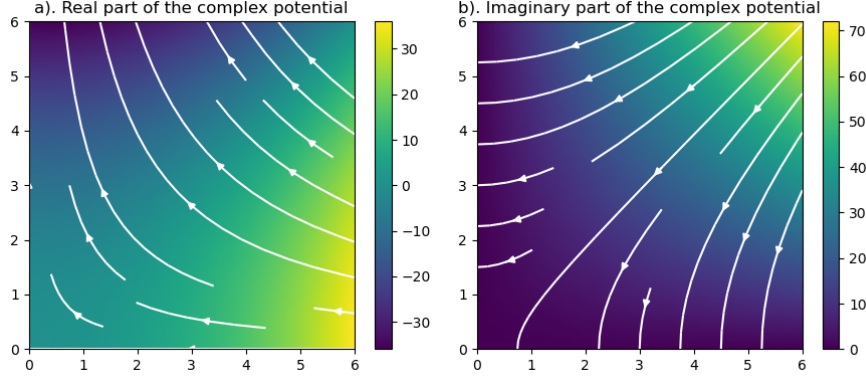


Figure 4: Real and imaginary parts of the complex potential z^2 . The streamlines in (a) show the direction of the magnetic potential, which is equal to the gradient of a . The streamlines in (b) show the directions of the equipotential lines.

If we now consider a complex potential \mathcal{A} , and an analytic mapping $f(z)$ from \mathcal{S} (the z -plane) onto co-domain \mathcal{S}' (the w -plane) with $f(z) \neq 0$ on \mathcal{S} . Now following theorem 7, if $\Delta_{x,y}\mathcal{A} = 0$, then so is $\Delta_{u,v}\mathcal{A} = 0$. Also:

$$\overline{\tilde{H}(z)} = \frac{d\mathcal{A}}{dz} = \frac{d\mathcal{A}}{dw} \frac{dw}{dz} = \overline{H(w)} f'.$$

And therefore also:

$$H(w) = \frac{\tilde{H}(z(w))}{f'(z(w))}, \quad (9)$$

and

$$\overline{H(w)} = \frac{1}{f'(z(w))} \frac{d\mathcal{A}(z(w))}{dz}. \quad (10)$$

Equations 9 and 10 are the key to solving boundary value problems using conformal mappings. They tell us we can calculate the magnetic field in a transformed plane if we know the derivative of the mapping (f'), inverse ($z(w)$), and either the original magnetic field (\tilde{H}) or the original complex potential (\mathcal{A}). Furthermore theorem 2.2 shows us that the newfound magnetic field obeys the Laplace equations if the original magnetic field did as well.

For our last electromagnetic bit of theory, we look at the magnetic field from an infinitely long wire carrying current into (or out of) the plane. As shown in textbooks, the scalar potential becomes:

$$a(x, y) = \frac{I}{2\pi} \tan^{-1} \left(\frac{y}{x} \right) = -\frac{I}{2\pi} \theta. \quad (11)$$

Here θ is the angle between the current filament and $z = x + iy$. To create our complex potential we look at the Cauchy-Riemann equations (5) in polar coordinates:

$$\begin{aligned} u_r &= \frac{1}{r} v_\theta, \\ v_r &= -\frac{1}{r} u_\theta. \end{aligned} \quad (12)$$

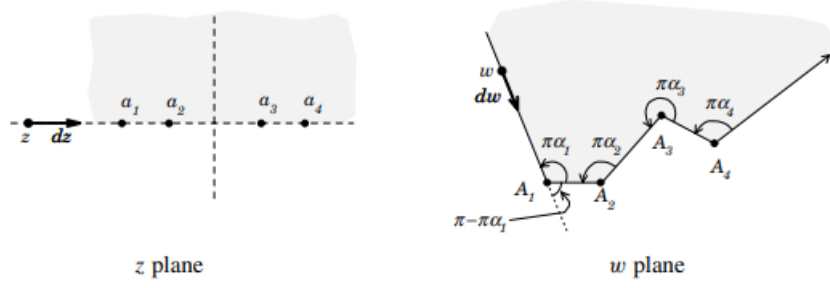


Figure 5: Transformation of a polygon from *complex variables* by *Mark J. Ablowitz and Athanassios Fokas*[13]

Since clearly $a_r = 0$ and $a_\theta = -\frac{I}{2\pi}$. Thus (up to a constant) $b = \frac{I}{2\pi} \log r$ and our complex potential becomes:

$$\mathcal{A} = \frac{I}{2\pi} (i \log r - \theta) = \frac{I}{2\pi} (i \text{Log} r e^{i\theta}) = \frac{I}{2\pi} i \text{Log} z. \quad (13)$$

Where we used $z = r e^{i\theta}$ and Log is the complex logarithmic function on the prime branch $\theta \in [0, 2\pi)$.

2.2.1. Schwarz–Christoffel

The Schwarz-Christoffel transformation explains how you can transform the upper z plane to any polygonal shape you want. It is given without proof below, cited as done in *Complex variables* by *Mark J. Ablowitz and Athanassios Fokas*[13], where you can also find a detailed proof.

Theorem 2.4 (Schwarz-Christoffel). *Let Γ be a piecewise linear boundary of a polygon in the w -plane, and let the interior angles at successive vertices be $\alpha_1\pi, \alpha_2\pi \dots \alpha_n\pi$. The transform defined by the equation*

$$\frac{dw}{dz} = \gamma (z - a_1)^{\alpha_1 - 1} (z - a_2)^{\alpha_2 - 1} \dots (z - a_n)^{\alpha_n - 1} \quad (14)$$

where γ is a complex number and a_1, \dots, a_n are real numbers, maps Γ into the real axis of the z plane. The vertices of the polygon, A_1, \dots, A_n are mapped to the points a_1, \dots, a_n on the real axis. The map is an analytic one-to-one conformal transformation between the upper half z plane and the interior of the polygon.

The notation in the theorem is also shown in figure 5.

Below an example is given where it becomes clear how the polygon can be created.

Example 1. Consider the conformal mapping given by $\frac{dw}{dz} = (z + 1)^{-1/2} z^{1/2}$. If we then take the integral $\int^z \frac{dw}{dz}(z') dz'$ with constant $\alpha \in [0, 2]$ on the domain $\mathcal{S} = \{z \mid a, b > 0\}$. When considering the real axis where $x < -1$, both $x + 1$ and x are negative, and thus the direction $\frac{\hat{dw}}{dz} \rightarrow (-1)^{-1/2} (-1)^{1/2} = \hat{i}$. Thus when moving on the real axis of the z -plane left of $x = -1$ to the right, we will move to the right in the w -plane. For $x \in (-1, 0)$, $z - 1$ changes sign and $\frac{\hat{dw}}{dz} \rightarrow (1)^{-1/2} (-1)^{1/2} = \hat{i}$, thus we will be moving upward (as if having turned $1/2 \pi$ rad upward). Lastly, for $x > 0$ in the z plane, our direction becomes \hat{i} again, and we move to the right again in the w plane.

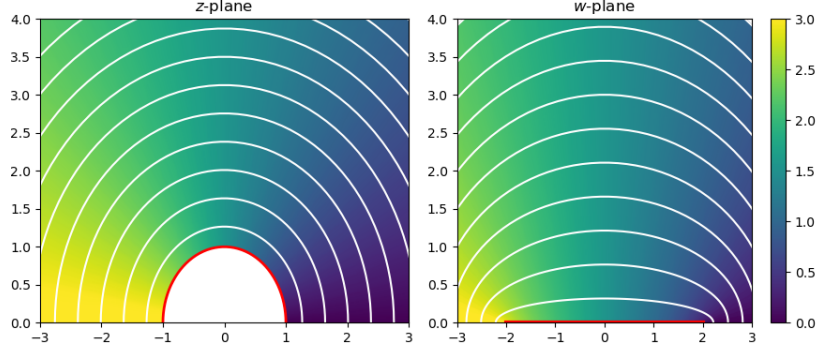


Figure 6: Joukowski mapping given by equation 15. Maps the positive real plane outside of the unit circle in z to the positive real plane in w . The red line shows the upper unit circle and its image, this image in the w plane will be the superconductor in many problems to come. The color map is the real part of the potential given by equation 27.

2.2.2. Joukowski mapping

The Joukowski mapping maps the upper complex plane outside of the unit circle in the z - plane to the upper complex plane in the w plane. It is given by:

$$f(z) = z + \frac{1}{z} \quad (15)$$

This mapping has three useful attributes. First, it maps the unit circle in the z -plane to $(-2,2)$ in the w -plane. This can be shown by substituting $z = e^{i\theta}$ for $\theta \in (0, \pi)$ in equation 15, and recognizing $e^{i\theta} + e^{-i\theta} = 2 \cos \theta$. Secondly, it maps the real axis outside of the unit circle $z \in \{x \in \mathbb{R} \mid |x| > 1\}$ to the real axis outside of our superconductor $w \in \{x \in \mathbb{R} \mid |x| > 2\}$. The last attribute is that $\lim_{|z| \rightarrow \infty} w(z) = z$, which is easily seen by taking the limit of equation 15. The derivative and inverse of our mappings are required and given by:

$$f'(z) = 1 - \frac{1}{z^2}, \quad (16)$$

$$z(w) = f^{-1}(w) = \frac{1}{2} \left(w + \sqrt{w^2 - 4} \right). \quad (17)$$

respectively. This shows our mapping is conformal on our domain, since the only two places where $f' = 0$ are $z = \pm 1$, which are on our border and not on our open domain.

3. Applications

Equipped with our theory on superconductors and conformal mappings we will look at applications of increasingly complex degree. In all applications, we assume a superconducting sheet where current moves into the page to shield a magnetic field. This shielded current is either due to an applied field in the y -direction or due to current moving through our sheet. We will first look at the situation in which the B -field due to an applied field or bias current is completely expelled from the sheet. We will see, however, that these solutions become non-physical since they imply singularities in the current distribution J through the wire. After these applications, we look at perfect screening of thicker slabs, where we cannot neglect the height of the sheet, these will make heavy use of Schwarz-Christoffel mappings and show ways of calculating magnetic field around any polygonal symmetries.

After the applications for infinite screening, we will cap the maximum current densities at a critical current density J_c . This necessitates flux penetration in these capped areas but gives us beautiful analytic solutions to our problems. Then we will look at hysteresis, which shows that the current distribution of a superconductor is not only dependent on its current state but also on its history. Lastly, we take a look at the combination of an applied field and bias current.

All parts of this section follow a certain chronological order, and I do not recommend skipping parts, since there will be a lot of referencing the previous sections. The only 'stand-alone' section is for the thick slabs perfectly shielding magnetic fields.

3.1. Complete screening of an applied magnetic field over a thin sheet

Consider an infinitely thin superconducting strip. Zero field cooled (ZFC) to under the superconducting critical temperature (T_c). Now we have our superconductor in the 'virgin state' (without any current or trapped magnetic flux). We then apply a small magnetic field perpendicular to the strip, and currents will flow through our strip to keep the field inside zero. Around the superconductor, the magnetic field will still obey Laplace's equations (equation 3). This situation is schematically shown in figure 7.

We see the real axis functioning as a mirror, and by symmetry, no magnetic field lines should cross it. It is therefore allowed (and as we'll see, also easier) to look at only the domain above the real axes. The superconductor itself also gives us boundary conditions, and must therefore also be taken out of the domain, giving us the domain: $\mathcal{D} = \{w \mid \text{Im}(w) > 0\} \setminus \{ti \mid t \in (0, a]\}$. This all results in the following boundary value problem:

$$\Delta \mathcal{A}(w) = 0 \quad z \in \mathcal{D} \quad (18a)$$

$$\lim_{|w| \rightarrow \infty} H(w) = H_0 \quad w \in \mathcal{D} \quad (18b)$$

$$\text{Im}(H(w)) = 0 \quad w \in \{t \mid t \in (-\infty, \infty)\} \quad (18c)$$

$$\text{Re}(H(w)) = 0 \quad w \in \{ti \mid t \in (0, a]\} \quad (18d)$$

Here $H(w)$ is the magnetic field in complex coordinates (with the real part as x -component, and imaginary part as y -component) at w (with again the real part as x -component, and imaginary part as y -component), a is the half-width of our superconductor, \mathcal{D} the domain as defined in the previous paragraph, H_0 the applied magnetic field, and t a real parameter. Note that

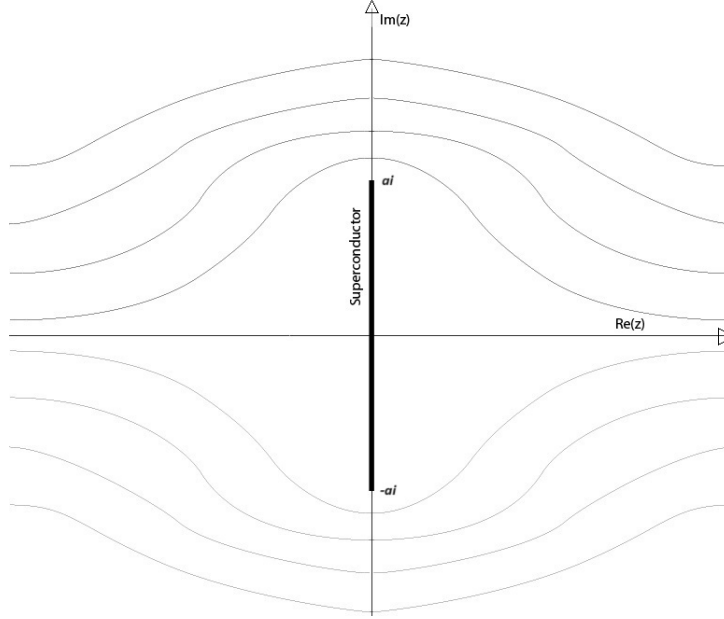


Figure 7: Schematic picture of our first example. The superconducting strip is shown in black in the middle, the magnetic streamlines are shown moving from left to right. The currents in the superconductor result in no penetration of the magnetic field through the superconductor. The superconductor has a width of $2a$.

the applied magnetic field H_0 is a real constant since the magnetic field is directed in the x -direction (or real-direction). Equation 18a is a result of the propagation of magnetic field in free space (that is: space free of net-charge or current), and is a direct consequence of the Maxwell equations as described in many electromagnetism textbooks [14]. Equation 18b, 18c, and 18d are the boundary conditions due to the applied field, symmetry axis, and infinitely shielding superconductor respectively.

We can solve the boundary value problem with the Schwarz-Christoffel mapping from a z -plane to our w -plane shown in figure 8. We first map to the specific case where $a = 1$, and then a simple adjustment will show the general solution. When choosing a magnetic field parallel to the real axes in the z -plane, we get a transformed magnetic field parallel to the real axis and the superconductor in the w -plane and thus satisfying equations 18c and 18d. As shown in section 2.2, equation 18a holds if the field in the z -plane is Laplacian, and the mapping is conformal (which Schwarz-Christoffel transformations always are). Equation 18b we will check last and show also holds. Then we know we have found the solution to our boundary condition.

The magnetic field in the z -plane that will give us our solution is H_0 everywhere:

$$\tilde{H}(z) = H_0 \quad (19)$$

According to Schwarz-Christoffel we get the following $f'(z)$ for $a_1 = -1$, $a_2 = 0$, $a_3 = 1$, $\alpha_1 = -1/2$, $\alpha_2 = 1$, and $\alpha_3 = -1/2$:

$$f'(z) = (z-1)^{-\frac{1}{2}} z (z+1)^{-\frac{1}{2}} = \frac{z}{(z^2-1)^{\frac{1}{2}}} \quad (20)$$

Integrating this equation gives us our mapping:

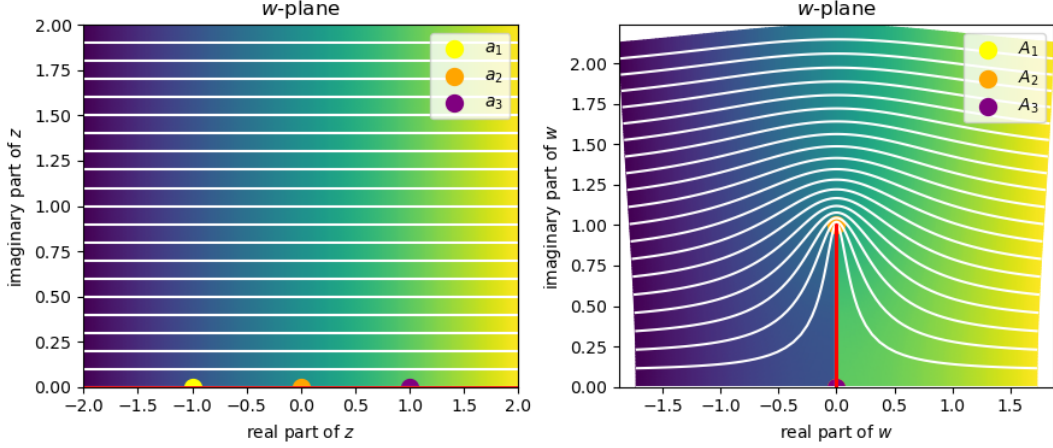


Figure 8: Schwarz-Christoffel mapping used to calculate magnetic field around an infinitely thin infinitely shielding superconductor. According to the notation of equation 14 we got $a_1 = -1$, $a_2 = 0$, $a_3 = 1$, $\alpha_1 = 1/2$, $\alpha_2 = 2$, and $\alpha_3 = 1/2$. Note that a_1 , and a_3 map to the same point in the w -plane, and the dots therefore overlap. The color map is the real part of the potential of the magnetic field given in equation 19.

$$f(z) = \int_{-1}^z f'(\hat{z}) d\hat{z} = \sqrt{z^2 - 1} = w(z) \quad (21)$$

Note that we integrate from $z = -1$ to ensure $f(-1) = 0$, as shown in figure 8 (integrating from 1 would have given us the same result). Taking the inverse gives an expression for w as a function of z :

$$z(w) = f^{-1}(w) = \sqrt{w^2 + 1} \quad (22)$$

Now applying equations 19, 20, and 22 into equation 9 gives us an expression for the magnetic field around a superconductor with $a = 1$:

$$\overline{H_{a=1}(w)} = \frac{w}{\sqrt{w^2 + 1}} H_0 \quad (23)$$

This equation is for $a = 1$. To introduce a you can simply map equation 23 to:

$$\overline{H_{\perp}(w)} = \frac{\frac{w}{a}}{\sqrt{\left[\frac{w}{a}\right]^2 + 1}} H_0 = \frac{w}{\sqrt{w^2 + a^2}} H_0 \quad (24)$$

Taking the limit $\lim_{|w| \rightarrow \infty} H_{\perp}(w)$ easily shows that equation 18b holds. Thus this equation solves our boundary value problem. We have called this H_{\perp} because from now forth we will be using mappings that end with results $\pi/2$ rad turned. Thus we want to make one final adjustment $w \rightarrow -iw$ to rotate our solution, giving:

$$\overline{H(w)} = \frac{-iw}{\sqrt{(-iw)^2 + a^2}} H_0 = \frac{iw}{\sqrt{w^2 - a^2}} H_0 \quad (25)$$

Equation 25 is visualized in figure 9. We also used simple mirroring to get the magnetic field in the other half of the complex plane. Furthermore, we have plotted the real, complex, and

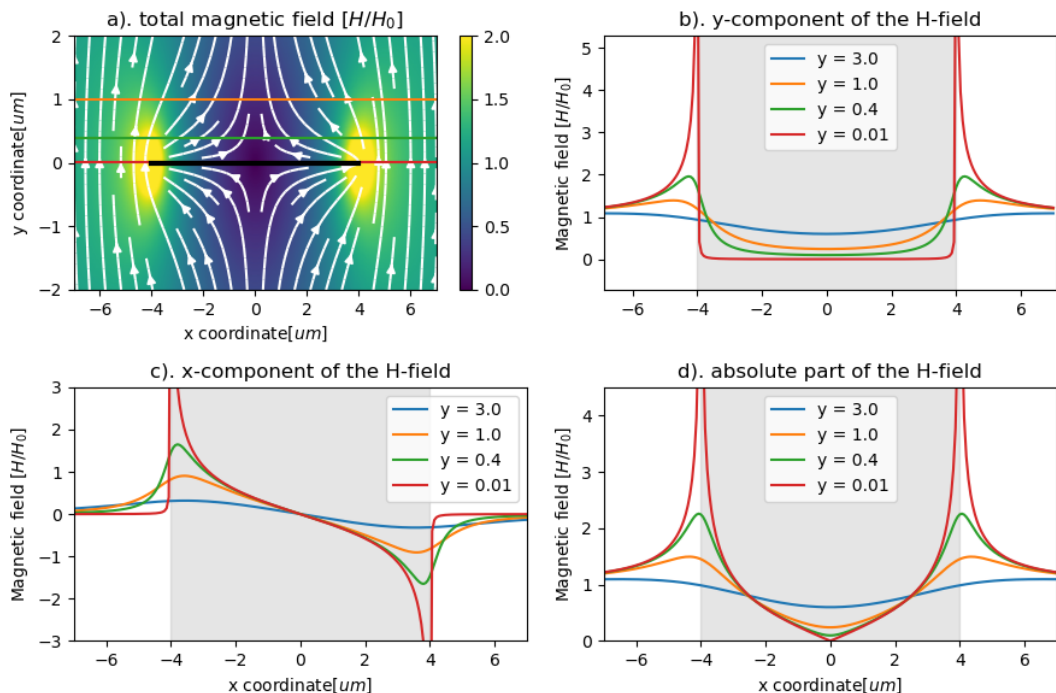


Figure 9: Plot of an infinitely shielded magnetic field around a thin superconducting sheet (equation 25) with $a = 4um$ and $H_0 = 1$. In (a) we show a colormap of the absolute values of the magnetic field H together with streamlines showing the direction of H , together they contain all information of the equation. We zoom in on the colored lines parallel to the superconductor to better understand our magnetic field. In (b) we show the y-component of the magnetic field on our parallel lines, which correspond to the imaginary part of our results. (c) shows the x-component of our field, which corresponds to the real part of our equation. (d) shows the absolute values of the magnetic field.

absolute parts of the magnetic field at multiple distances from the superconducting sheet. In 9b we show the y-component of the magnetic field on our parallel lines. The red line approaching zero close to the superconductor shows perfect magnetic field screening. The blue line tends to H_0 , which is expected by equation 18b. 9c shows the x-component of our field. According to appendix C we know that the red line approximates the current distribution inside the superconductor. Here the non-physical singularities happen at the edges of the superconductor.

Our solution for perfect shielding has two singularities at the edge of the sheet (at $w = \pm i$). As explained in appendix C, the current distribution would also become infinite. This is (apart from non-physical) not realistic since the superconductor has a maximum current density (J_c) above which the superconductivity breaks down. After turning on the magnetic field slightly, the edges will instantly reach this critical current density. Because this differs from the distribution for perfect shielding, we can conclude that the magnetic field penetrates the edges of the sheet. This situation is also analytically solvable and will be done so in section 3.5. For low magnetic fields this penetration of the magnetic field is very small, and our equation 25 gives a good approximation for the magnetic field around the sheet (as we shall see in section 4.

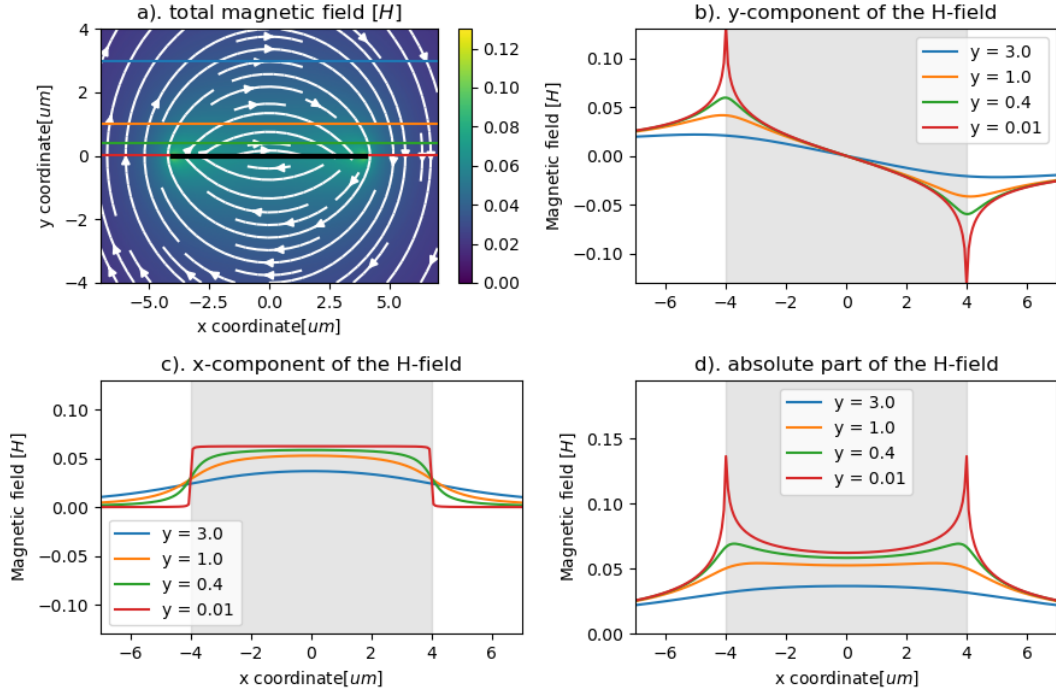


Figure 10: Magnetic field around a normal conducting sheet carrying a current (equation A22, with $I = 1$ and $a = 4$). As usual, the red line in 10c is proportional to the current distribution, and shows our assumed uniformity.

3.2. Complete screening of a magnetic field magnetic due to bias current through a thin sheet

In the previous subsection, we looked at the magnetic field around a superconductor resulting from an applied magnetic field. We got the theoretical solution for perfect screening of the magnetic field, with its non-physical singularities. Now we shall look at how the magnetic field around the sheet becomes after applying a bias current through it. In a normal conducting sheet, the resistance per area increases with the current distribution. Current follows the path of least resistance, and therefore we would expect the current distribution to be uniform. Appendix D explains how to calculate the magnetic field around a normal sheet, and this result is plotted in figure 10.

As you can see in 10b, the magnetic field penetrates the normal conductor. If a small current is applied through a superconductor, the current will distribute in a specific way to cancel the magnetic field created by the current itself. For perfect shielding then: the magnetic field flows parallel over the surface. We then get the following boundary conditions over the domain $\mathcal{D} = \{z \in \mathbb{C} \mid \text{imag}(z) > 0\}$:

$$\Delta \mathcal{A}(w) = 0 \quad w \in \mathcal{D} \quad (26a)$$

$$\lim_{r \rightarrow \infty} \int_0^\pi H(re^{i\theta}) d\theta = \frac{I}{2} \quad w \in \mathcal{D} \quad (26b)$$

$$\text{Im}(H(w)) = 0 \quad w \in \{t \mid t \in (-a, a)\} \quad (26c)$$

$$\text{Re}(H(w)) = 0 \quad w \in \{t \mid t \in (-\infty, -a) \cup (a, \infty)\} \quad (26d)$$

Equation 26a again describes the propagation of a magnetic field in free space. 26b makes use of Amperes law (equation A19) to ensure the current through the superconductor is equal to I . 26c and 26d are due to the superconductor not being penetrated, and by symmetry respectively.

We shall make use of the Joukowski mapping as shown in figure 6. This mapping is given by equation 15, with equation 16 and 17 its derivative and inverse respectively. The sheet in the w plane will be mapped from the upper half unit circle in the z plane. We can easily find a potential field that has parallel components on the upper unit circle, namely the potential a current filament at $z = 0$ would have (13):

$$\begin{aligned} \tilde{A}(z) &= \frac{I}{2\pi} i \text{Log}(z) \\ \tilde{H}(z) &= \frac{d\tilde{A}}{dz} \\ &= \frac{I}{2\pi} \frac{i}{z} \end{aligned} \quad (27)$$

This is the same potential and field you would get for a current filament at the point $(0, 0)$ in the z -plane (note that this is outside our boundary). Therefore we can use Amperes law (equation A19) and the fact that $\lim_{|z| \rightarrow \infty} w(z) = z$, to conclude equations 26a and 26b hold in the w -plane. Also, since the direction of our magnetic field is $\hat{\theta}$, we know it is parallel to the unit circle in the z -plane, and (because conformal mappings are angle-preserving by definition) also parallel to the 'superconductor' occupying $(-2, 2)$ in the w -plane (equation 26c with $a = 2$). By symmetry the magnetic field is also perpendicular to the real axis, satisfying equation 26d (with $a = 2$). Finally, combining equations 27, 16, and 17 and plugging this in equation 9 we can find the magnetic field for $a = 2$:

$$\overline{H_{a=2}(w)} = \frac{I}{2\pi} \frac{\sqrt{w^2 - 4} + w}{w\sqrt{w^2 - 4} + w^2 - 4} i = \frac{I}{2\pi} \frac{1}{\sqrt{4 - w^2}} \quad (28)$$

Where the simple map $(I, w) \rightarrow (2I/a, 2w/a)$ to get the solution for a general w :

$$\overline{H(w)} = \frac{I}{2\pi} \frac{1}{\sqrt{a^2 - w^2}} \quad (29)$$

This equation is visualized in figure 11. The same problem we got for infinite magnetic screening arises with our new solution: two singularities at the edges of our sheet ($w = \pm a$). As per the same argumentation, we will cap our edges at a critical current density J_c , and assume only perfect shielding within the areas of critical current. This will be done in section 3.6.

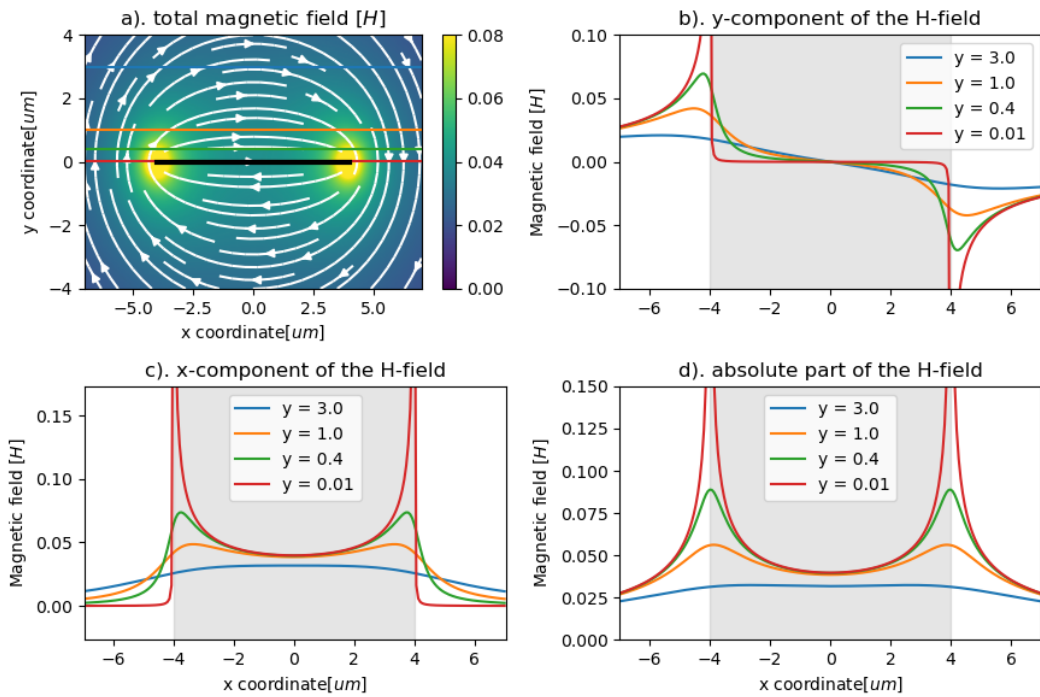


Figure 11: Magnetic field around a superconductor with a current running through (equation 29, also mirrored in the real-axis using equation A20 to incorporate the whole of \mathbb{C}). (a) shows a heat map of the absolute magnetic field. (b) takes the imaginary part, which equals our y -component. (c) takes the real part and thus x -component. The red curve in (c) is therefore also proportional to the current distribution (appendix 31), which shows our non-physical singularities in the current distribution.

3.3. Complete screening of an applied magnetic field over a thick sheet

In the previous two sections, we calculated the magnetic field around an infinitesimally thin superconducting sheet subject to respectively a magnetic field on, or current through it. In this section and the next, we will show how we can perfectly shield the magnetic field if we cannot afford to neglect the height of the sheet.

For both applications, we use a similar Schwarz-Christoffel mapping. For an applied magnetic field we look at the mapping shown in figure 12. Here we see a mapping transforming our upper z -plane to a domain where the superconducting sheet is taken out. By symmetry, we know that the magnetic field should not penetrate the x -axis, and due to the superconductors boundary conditions, we know it cannot penetrate the superconductor as well. If we then take a simple magnetic field that is parallel to the real axis and use this mapping we know that the magnetic field stays parallel to the real axis and the superconductor. The Schwarz-Christoffel equation (eq 14) becomes:

$$\frac{df}{dz} = \frac{(z^2 - 1)^{1/2}}{(z^2 - 4)^{1/2}} \quad (30)$$

where we took $n = 4$, $\gamma = 1$, $a_1 = -2$, $a_2 = -1$, $a_3 = 1$, $a_4 = 2$, $\alpha_1 = 1/2$, $\alpha_2 = 3/2$, $\alpha_3 = 3/2$, and $\alpha_4 = 1/2$ in equation 14. This equation is sadly not analytically integrable, and therefore we look at numerical solutions in this section. Integrating yields (up to a constant):

$$f(z) = \int^z dz' \frac{(z'^2 - 1)^{1/2}}{(z'^2 - 4)^{1/2}} \quad (31)$$

Which we have to solve numerically. To solve equation 9 we only now need the inverse mapping. This can be done using the Newton-Rhapson method (which is very effective since we have an analytic expression for the derivative). This method can be found in many textbooks about numerical analysis[15]. Our magnetic field in the z -plane is given again by equation 19. Plugging equations 19, 30, and our numerical approximation for f^{-1} into 9 gives us figure 13 (after turning it by $\pi/2$ rad for consistency among images). Here we are not able to conclude any easy methods for the current density, since section C and its results only work for infinitesimally thin sheets.

3.4. Complete screening of a magnetic field magnetic due to bias current through a thick sheet

We want to use a similar Schwarz-Christoffel mapping to calculate the magnetic field around a thick superconducting slab when applying a current. However, we must first make sure that the different boundary conditions hold in our previous z -plane. This is done by using the same Joukowski mapping as in the thin sheet example, and then mapping this new plane using the new Schwarz-Christoffel mapping. This method is shown in 14. The intermediate plane we label the u -plane. The Schwarz-Christoffel mapping from u to w we get from 14 with $n = 4$, $a_1 = -2$, $a_2 = -\sqrt{3}$, $a_3 = \sqrt{3}$, $a_4 = 2$, $\alpha_1 = 1/2$, $\alpha_2 = 3/2$, $\alpha_3 = 3/2$, and $\alpha_4 = 1/2$ we call $S(u)$:

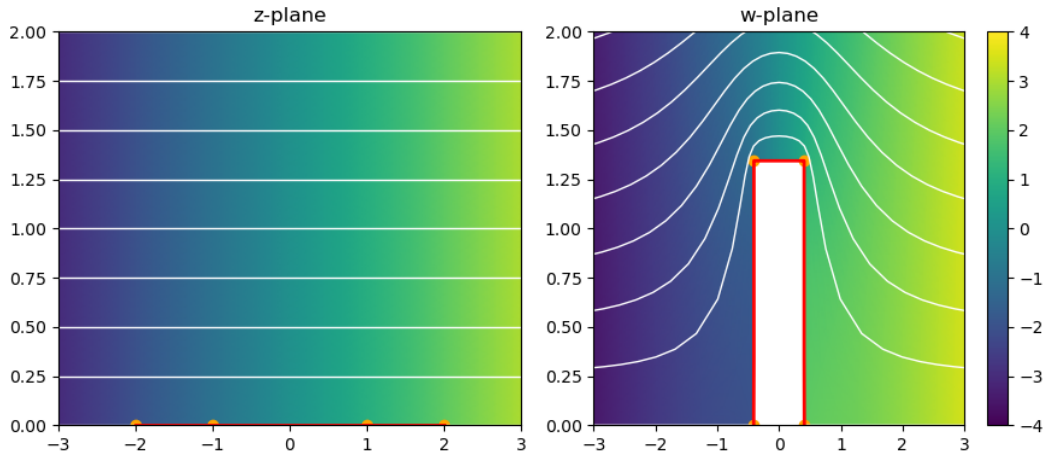


Figure 12: Schwarz-Christoffel mapping for calculating shielded magnetic field around a thick superconducting sheet. The mapping is given by equation 14 with $n = 4$, $a_1 = -2$, $a_2 = -1$, $a_3 = 1$, $a_4 = 2$, $\alpha_1 = 1/2$, $\alpha_2 = 3/2$, $\alpha_3 = 3/2$, and $\alpha_4 = 1/2$. Color map shows the real part of the potential.

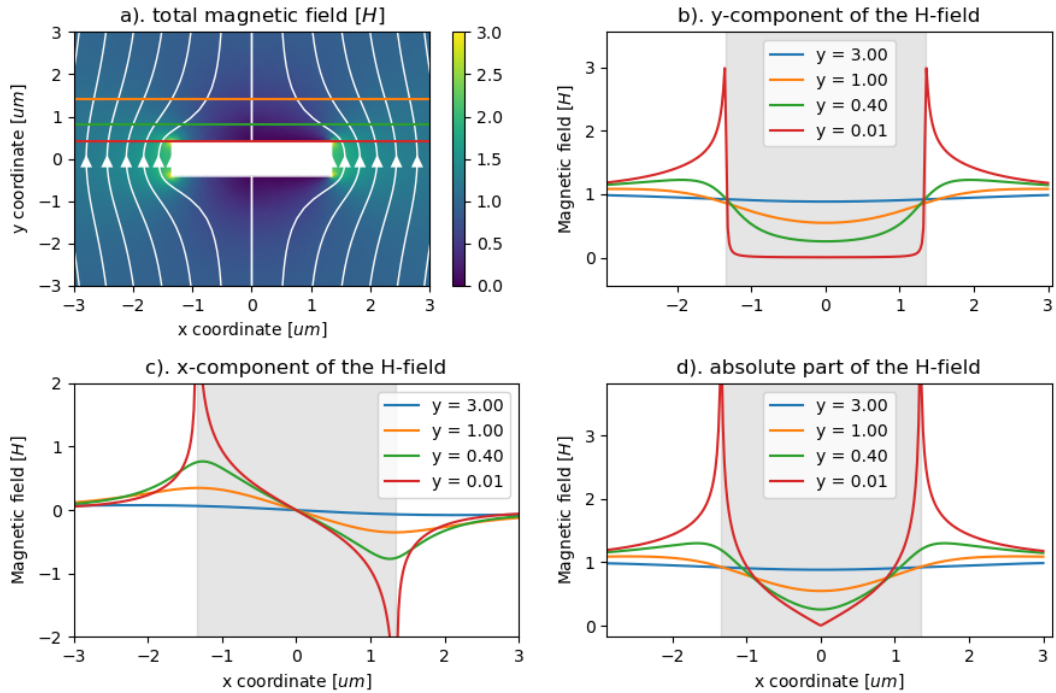


Figure 13: Magnetic field around a thick superconducting slab calculated from 19, 30, and the numerical inverse of equation 31. Rotated $\pi/2$ rad to keep consistency of plots and mirrored in the real-axis to complete the entire complex plane. b, c and d show the y-component, x-component, and absolute values at different heights respectively.

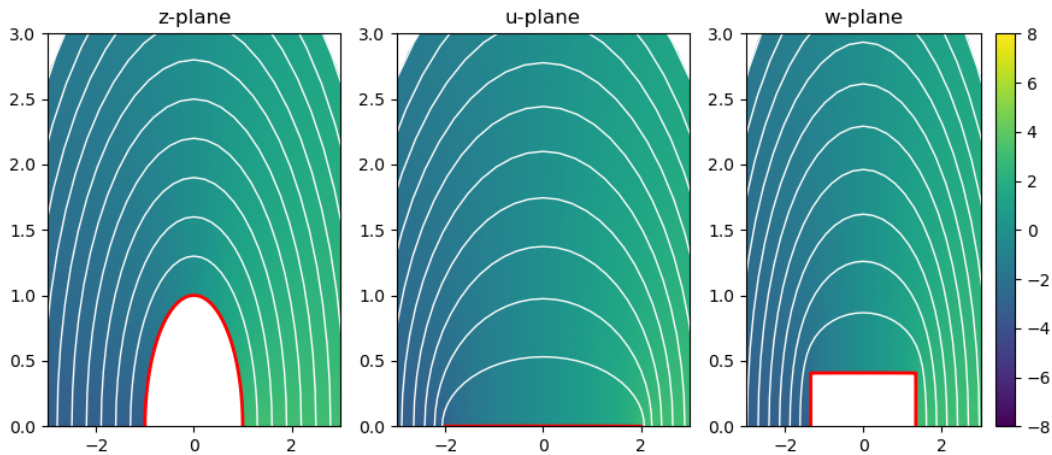


Figure 14: The double mapping used to calculate the magnetic field around a thick superconductor carrying a current. The red line symbolizes either the pre-image of the superconductor or the superconductor itself. The color map shows the real part of the magnetic potential.

$$S'(u') = \frac{(u'^2 - 3)^{1/2}}{(u'^2 - 4)^{1/2}} \quad (32)$$

$$S(u) = \int^u du' \frac{(u'^2 - 3)^{1/2}}{(u'^2 - 4)^{1/2}} \quad (33)$$

Defining $J(z)$ as the Joukowski mapping from the z plane to the u plane (equation 15, but with a different name to conserve f for the total mapping), we get:

$$f(z) = S(J(z)) \quad (34)$$

$$f'(z) = S'(J(z))J'(z) \quad (35)$$

$$f^{-1}(w) = J^{-1}(S^{-1}(w)) \quad (36)$$

using the chain rule for derivatives and the 'socks and shoes' rule for the inverses of a compound function. Here S^{-1} and S are numerical, but S' is exact. Plugging these functions into 9 with our original \mathcal{A} again equal to 27 gives us the plots in figure 13.

It is valuable to realize the strength of the Schwarz-Christoffel mappings. Any shape of a superconductor can be made using this equation, and from that (and a symmetry axis) we can calculate the magnetic field around it after applying either a magnetic field onto it, or a current through it.

3.5. Partial screening of applied magnetic field over a thin sheet

Our solutions for perfect shielding of a magnetic field are good approximations for small fields (as we shall see when looking at our results). For higher fields, they start to lose accuracy. To approximate the field around a superconductor for higher magnetic fields, we will consider a maximum current density through the superconductor, above which no superconducting currents can flow anymore. We call this the critical current density J_c . For an applied magnetic

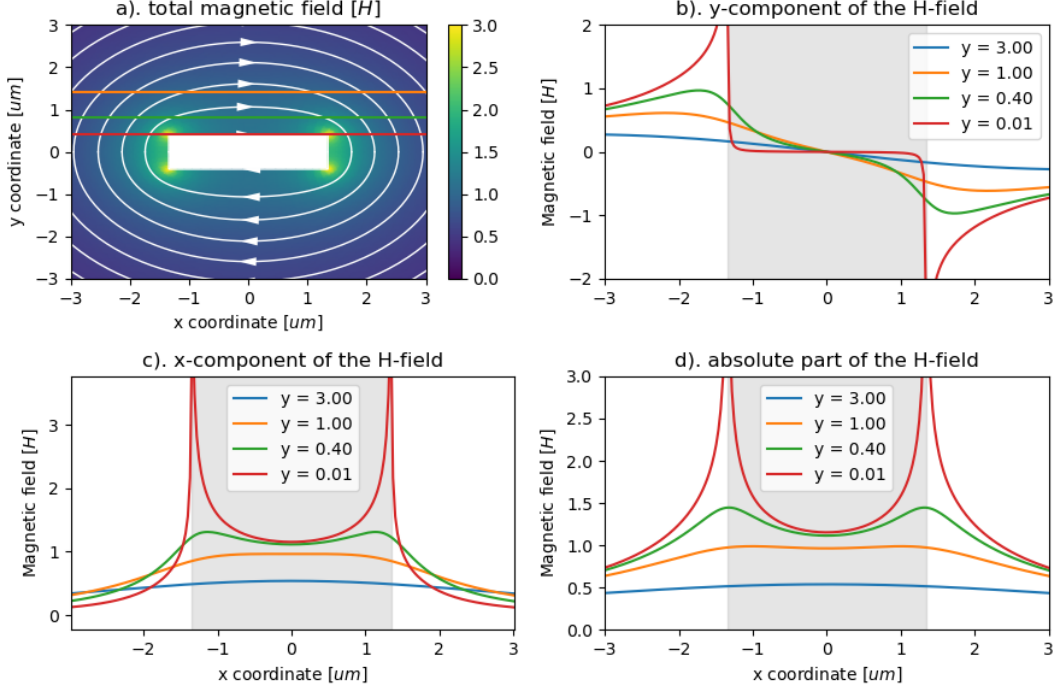


Figure 15: Field around superconducting thick slab with current going through it. Calculated by plugging equations 35, 27 and our numerical approximations for 36 into eq 9, and mirroring in the real-axis to complete the complex plane.

field then, we see that the critical current density is reached first at the edges (equation 25 and figure 9), and we will cap it here. In the places where we cap our magnetic field, we will see magnetic flux penetrating. In the places where the critical current is not reached, we want no penetrating flux. We introduce the variable b , which shows the part of the superconductor not penetrated by magnetic flux. We view the upper complex plane as our domain $\mathcal{D} = \{w \mid \text{Re}(z) > 0\}$, place our superconductor from $(-a, a)$, and define our perfectly shielded region as $(-b, b)$. The applied magnetic field then becomes $H_0 i$, since it is directed in the y -direction. Our problem then becomes:

$$\Delta \mathcal{A}(w) = 0 \quad w \in \mathcal{D} \quad (37a)$$

$$\lim_{|w| \rightarrow \infty} H(w) = H_0 i \quad w \in \mathcal{D} \quad (37b)$$

$$\text{Im}(H(w)) = 0 \quad w \in \{t \mid t \in (-b, b)\} \quad (37c)$$

$$\text{Re}(H(w)) = J_c/2 \quad w \in \{t \mid t \in (-a, -b)\} \quad (37d)$$

$$H(w) = -J_c/2 \quad w \in \{t \mid t \in (b, a)\} \quad (37e)$$

$$\text{Re}(H(w)) = 0 \quad w \in \{t \mid t \in (-\infty, -a) \cup (a, \infty)\} \quad (37f)$$

The 'new' boundary conditions 37d and 37e are due to the edges reaching J_c in the fashion of figure 9, and the relation between magnetic field and current density from equation A21. We tackle this problem by shielding the current through the lines $|x| \in (b, a)$ in the perfectly shielded region $(-b, b)$. In appendix A, we explain how to shield a current filament such that it does not penetrate a predetermined sheet. We consider constant current density in the sheet

parts from $(-a, -b)$ and (b, a) as integrals over current filaments. We take equation A10 and consider a current filament at x of strength $J_c dx$ somewhere in (b, a) . At $-x$ there will be a current filament $-J_c dx$. Combination of these two current filaments in our mirroring equation would become:

$$\begin{aligned}\overline{H_{Jdx}(w; x)} &= \frac{J_c \sqrt{x^2 - b^2} i}{2\pi \sqrt{w^2 - b^2}} \left(\frac{dx}{(w - x)} - \frac{-dx}{(w + x)} \right) \\ &= \frac{w \sqrt{x^2 - b^2} i}{\pi \sqrt{w^2 - b^2} (w^2 - x^2)} J_c dx\end{aligned}\quad (38)$$

Here $\overline{H_{Jdx}(w; x)}$ is the magnetic field at w due to screening of the current filaments Jdx and $-Jdx$ at x and $-x$ respectively. We want to integrate this function from b to a to shield our sheet current, however, we will still see two singularities pop up:

$$\begin{aligned}\overline{H_1(w)} &= \frac{w}{\sqrt{w^2 - b^2}} \frac{J_c i}{\pi} \int_b^a \frac{\sqrt{x^2 - b^2}}{w^2 - x^2} dx \\ &= \frac{w}{\sqrt{w^2 - b^2}} f(w)\end{aligned}\quad (39)$$

These singularities are at $w \in \{b, -b\}$. We recognize equation 25 as the exploding first term of 39 but with thickness b . We define $f(w)$ as the second part of our equation. To get a solution without singularities we can take a superposition of equations 39 and 25 (with thickness b) since they both allow no flux to penetrate through the region $(-b, b)$. In other words: we can add an equation of the form $w/\sqrt{w^2 - b^2}$. Our problem now becomes finding an F independent of w such that:

$$H_1 - \frac{w}{\sqrt{w^2 - b^2}} F = \frac{w}{\sqrt{w^2 - b^2}} (f(w) - F) \quad (40)$$

has no singularities anymore. We can do this since both equations allow no flux to penetrate the shielded area $(-b, b)$, and the superposition of both will not be as well. Of course, this equation can only be without singularities if $f(\pm b) - F = 0$, and thus we will try $F = f(\pm b)$. From 39 it immediately becomes clear that:

$$\begin{aligned}f(\pm b) &= \frac{J_c i}{\pi} \int_b^a \frac{\sqrt{x^2 - b^2}}{b^2 - x^2} dx \\ &= F\end{aligned}$$

Where F is called a singularity intensity factor. Now for our full solution we subtract $Fw/\sqrt{w^2 - b^2}$ from $\overline{H_1}$, giving:

$$\begin{aligned}\overline{H(w)} &= \frac{J_c i}{\pi} \frac{w}{\sqrt{w^2 - b^2}} \int_b^a \sqrt{x^2 - b^2} \left(\frac{1}{w^2 - x^2} - \frac{1}{b^2 - x^2} \right) dx \\ &= \frac{J_c i}{\pi} \frac{w}{\sqrt{w^2 - b^2}} \int_b^a \sqrt{x^2 - b^2} \left(\frac{b^2 - w^2}{(w^2 - x^2)(b^2 - x^2)} \right) dx \\ &= \frac{J_c i}{\pi} w \sqrt{w^2 - b^2} \int_b^a \frac{1}{(w^2 - x^2) \sqrt{x^2 - b^2}} dx\end{aligned}\quad (41)$$

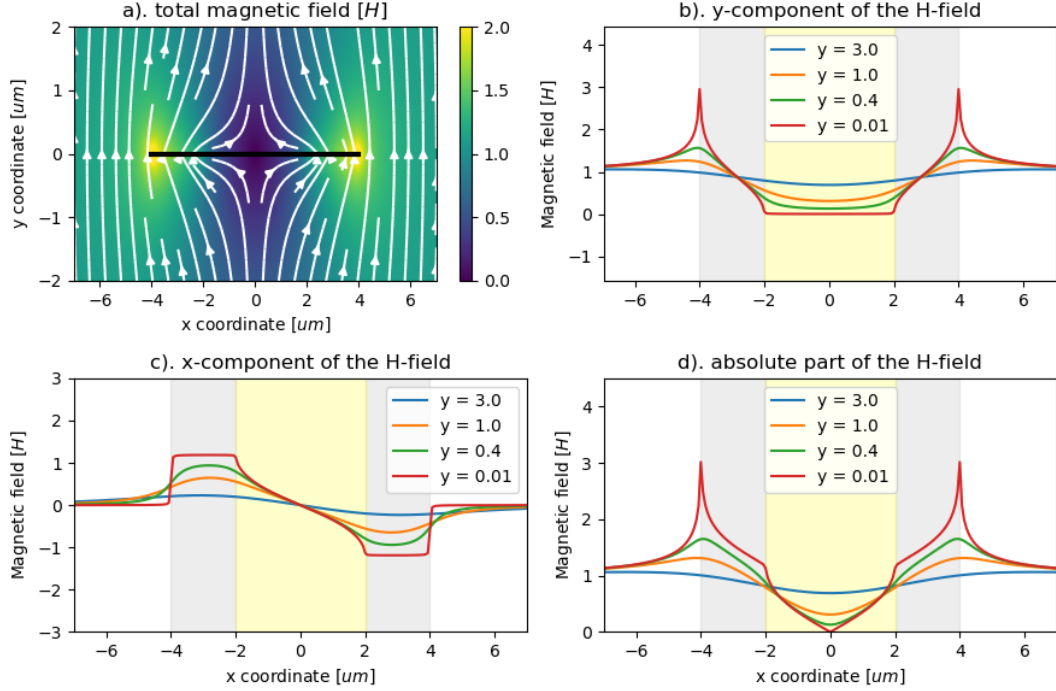


Figure 16: Plots of equation 42 with $b = 2$, $a = 4$, and $J_c = 2$. The colormap in a shows the absolute magnetic field strength with the direction shown by the stream plot. The areas perfectly shielded are shown in yellow in b, c, and d.

This integral solves into¹:

$$\begin{aligned}
 \overline{H(w)} &= \frac{J_c}{\pi} \tan^{-1} \left[\frac{x\sqrt{b^2 - w^2}}{w\sqrt{x^2 - b^2}} \right] \Bigg|_{x=b}^a, \\
 &= \frac{J_c}{\pi} \left(\tan^{-1} \left[\frac{a\sqrt{b^2 - w^2}}{w\sqrt{a^2 - b^2}} \right] - \frac{\pi}{2} \right)
 \end{aligned} \tag{42}$$

Where \tan^{-1} is the arctan or inverse of tangent. This is an extremely nice result for the magnetic field around a superconductor, which is shown in figure 16 for $J_c = 2$, and $b = 2$. You can recognize $J_c = 2$ by looking at the B_x plot very close to the superconductor (16c, the red curve), which should be half the critical current density at the interval $x \in (-a, -b)$.

We have defined one parameter too many at the beginning of our problem because the variables b , J_c , and H_0 are interdependent. For a given H_0 and J_c there is a single value b . We now have chosen a J_c and b , and therefore there is only a single value of H_0 possible. We can calculate that by realizing that only magnetic field was added as a result of subtracting $Fw/\sqrt{w^2 - b^2}$. The amount of magnetic field added this way can be taken from equation 25:

¹I will not be evaluating this integral in this paper, nor will I evaluate the similar integrals in the coming two sections. They are too long and beyond the scope/relevancy of this thesis. WolframAlpha gives a step-by-step guide to solve it when fed the prompt.

$$\begin{aligned}
\frac{Fw}{\sqrt{w^2 - b^2}} &= \frac{Fw}{\sqrt{w^2 - b^2}} iH_0, \\
F &= H_0 i, \\
\frac{J_c i}{\pi} \int_b^a \frac{\sqrt{x^2 - b^2}}{b^2 - x^2} dx &= H_0 i, \\
\implies H_0 &= \frac{J_c}{\pi} \cosh^{-1}(a/b)
\end{aligned} \tag{43}$$

Thus if we know H_0 , and J_c and want to calculate b we get:

$$b = a / \cosh \frac{H_0 \pi}{J_c} \tag{44}$$

3.6. Partial screening of a magnetic field due to current through a thin sheet

In solving perfect shielding of the magnetic field created by the current through a superconductor itself we also found singularities at the edges. We will follow the same steps as in the applied magnetic field case, with the only difference that initially, the charges at x , and $-x$ are of the same sign Jdx , since that are the signs our currents need to be capped in (see figure 11 and equation 29). Thus for shielding of current filaments of strength Jdx on x and x' , our shielding equation then becomes (from equation A10):

$$\begin{aligned}
\overline{H_{Jdx}(w; x)} &= \frac{J_c \sqrt{x^2 - b^2} i}{2\pi \sqrt{w^2 - b^2}} \left(\frac{dx}{w - x} + \frac{-dx}{w + x} \right) \\
&= -\frac{i J_c}{\pi} \frac{x \sqrt{x^2 - b^2}}{(w^2 - x^2) \sqrt{w^2 - b^2}} dx.
\end{aligned} \tag{45}$$

With the same notation as equation 38. Trying to integrate this will also lead to singularities at the edges:

$$\begin{aligned}
\overline{H_1(w)} &= \frac{-i J_c}{\pi} \frac{1}{\sqrt{w^2 - b^2}} \int_b^a \frac{x \sqrt{x^2 - b^2}}{(w^2 - x^2)} dx \\
&= \frac{1}{\sqrt{w^2 - b^2}} f(w)
\end{aligned} \tag{46}$$

Where we recognize again the equation for perfect shielding after applying current through a sheet of width b (equation 29 with $a = b$), and can subtract this to erase the singularity (without erasing our region not penetrated by flux). For this, we first find the singularity factor F in the same way as the magnetic shielding case:

$$\begin{aligned}
f(b) &= \frac{-i J_c}{\pi} \int_b^a \frac{x \sqrt{x^2 - b^2}}{(b^2 - x^2)} dx, \\
&= F.
\end{aligned}$$

Now subtracting $F/\sqrt{x^2 - b^2}$ from our equation 46 gives:

$$\begin{aligned}
\overline{H(w)} &= \overline{H_1(w)} - \frac{F}{\sqrt{w^2 - b^2}} \\
&= \frac{-iJ_c}{\pi} \frac{1}{\sqrt{w^2 - b^2}} \int_b^a x \sqrt{x^2 - b^2} \left(\frac{1}{w^2 - x^2} - \frac{1}{b^2 - x^2} \right) dx, \\
&= \frac{-iJ_c}{\pi} \frac{1}{\sqrt{w^2 - b^2}} \int_b^a x \sqrt{x^2 - b^2} \left(\frac{w^2 - b^2}{(w^2 - x^2)(x^2 - b^2)} \right) dx, \\
&= \frac{-iJ_c}{\pi} \sqrt{w^2 - b^2} \int_b^a \frac{xdx}{(w^2 - x^2)\sqrt{x^2 - b^2}}.
\end{aligned} \tag{47}$$

Evaluating the integral gives:

$$\begin{aligned}
\overline{H(w)} &= \frac{J_c}{\pi} \tan^{-1} \left[\frac{\sqrt{x^2 - b^2}}{\sqrt{b^2 - w^2}} \right] \Bigg|_{x=b}^a, \\
&= \frac{J_c}{\pi} \tan^{-1} \left[\frac{\sqrt{a^2 - b^2}}{\sqrt{b^2 - w^2}} \right].
\end{aligned} \tag{48}$$

Lastly, we want to calculate the total amount of current I we sent through our sheet. This can be shown to be[3]:

$$\begin{aligned}
I &= 2J_c \sqrt{a^2 - b^2} \\
b &= a \sqrt{1 - I^2/I_{\max}^2}
\end{aligned} \tag{49}$$

Here I_{\max} is the current when the entire sheet is carrying the critical current density and is easily calculated by $I_{\max} = 2aJ_c$. Equation 48 is visualized in figure 17. Here you recognize the capped current densities as the red curve in (c).

3.7. Hysteresis of the magnetic field around a superconducting for AC currents or applied magnetic fields

When applying alternating magnetic fields over or currents through a superconductor a rich variety of situations can happen. If we apply a magnetic field over the sheet, we see that we end in a situation where there is magnetic field trapped within the sheet (equation 42). As explained by Bean[8], if we now decrease the applied magnetic field, the superconductor will try to keep the trapped flux and shield the difference in magnetic field. Which is the difference between the field initially applied, and where it is decreased to. Luckily, we do not need to calculate this new shielding, since we have already calculated how our sheet shields the magnetic field in equation 42. There is only one difference: the sides of our superconductor are already at critical current density, and if it starts shielding it will go to the other sign of critical current density, which effectively puts our situation to one with double critical current density.

Now if we then increase the magnetic field to H_0 , and then decrease it to H_a (note that $H_a \in (-H_0, H_0)$)

$$H_{H,\downarrow}(w, H_a, J_c) = H_H(w, H_0, J_c) - H_H(w, H_0 - H_a, 2J_c). \tag{50}$$

Here $H_{H,\downarrow}(w, H_a, J_c)$ is the magnetic field as a function of w after increasing the field to H_0 , and then decreasing it to H_a , and $H_H(w, H, J_c)$ is the magnetic field as given in equation 42,

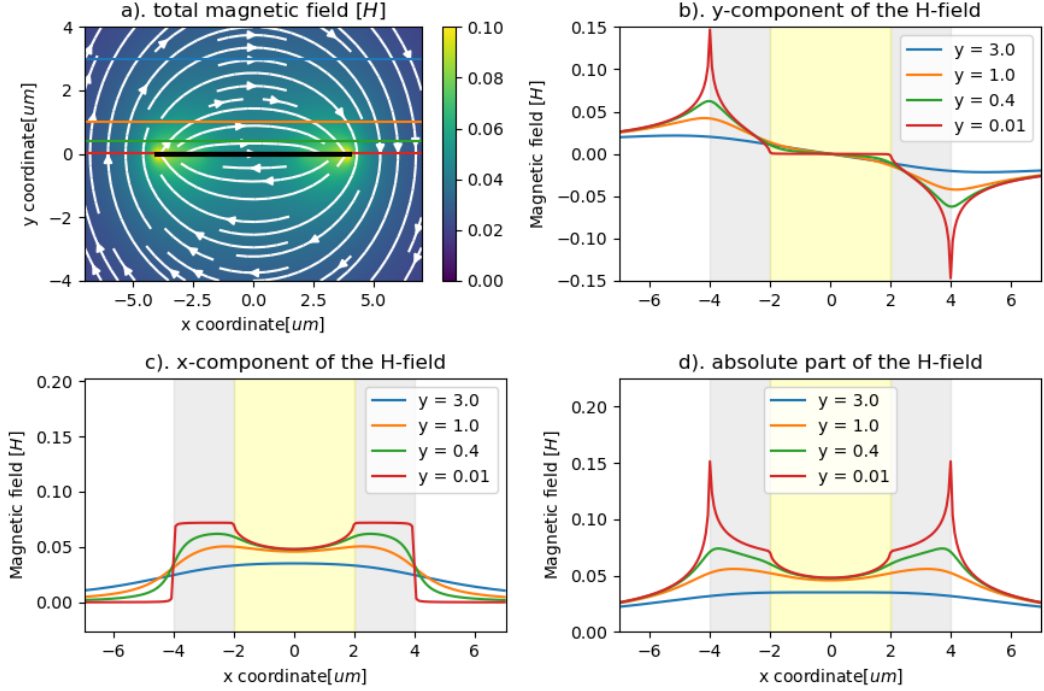


Figure 17: Plots of equation 48 with $b = 2$, $a = 4$, and $J_c = .15$. The colormap in a shows the absolute magnetic field strength with the direction shown by the stream plot. The areas perfectly shielded are shown in yellow in b, c, and d.

where we have substituted b from equation 43. Also for current running through the sheet, the same equation holds:

$$H_{I,\downarrow}(w, I_a, J_c) = H_I(w, I_0, J_c) - H_I(w, J_0 - J_a, 2J_c) \quad (51)$$

Where now again $H_{I,\downarrow}$ is the magnetic field as the current is decreased from I_0 to I_a , and H_I is taken from equation 48 with b substituted as per equation 49. Equations 50 and 51 are plotted for the magnetic field very close to the wire for different H_a , or I_a in figures 18 and 19 respectively.

In both figures, the color map shows the situation where either the bias current or applied magnetic field is turned off. You can see that there is still a field around a superconductor even after the applied field or netto current is decreased again to zero. If we now introduce the negative magnetic moment M of a system by:

$$M = \int_{-a}^a xJ(x)dx, \quad (52)$$

we see that in the symmetric situation of current, we get no magnetic moment ever. However, the asymmetric behaviour of the magnetic field yields magnetic moment even after the magnetic field is again switched off to zero. This is an explanation for the famous hysteresis plot of a superconductor shown in figure 20.

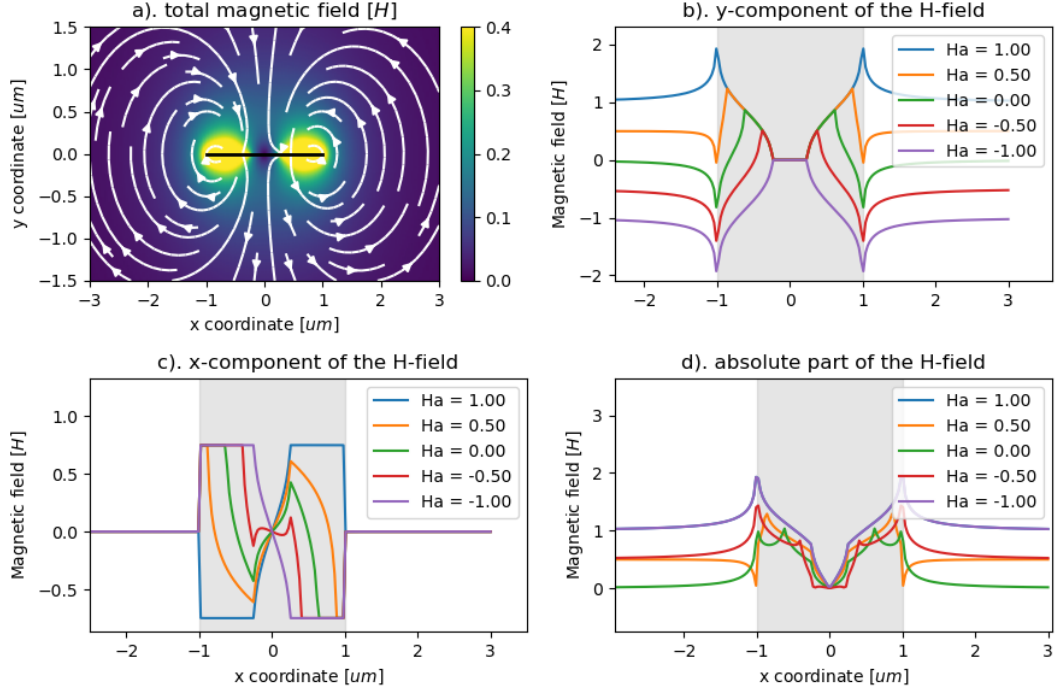


Figure 18: plot of 50 with $J_c = 1.5$, $H_0 = 1$, and varying H_a . The colormap in (a) is for the magnetic field on the intermediate step where $H_a=0$. The magnetic field in (b), (c), and (d) are taken very close to the real axis. (c) is also proportional to the current distribution in our sheet

3.8. Partial screening of an applied magnetic field and a magnetic field due current

For combining current and field, we will first look at a sheet located on the real axis from $(-b, a_1)$, shielding critical current density J_c on the interval (b, a_1) , where we want no penetrating flux in the interval $(-b, b)$. We again start with the shielding of a current filament $J_c dx$ at $x \in (b, a_1)$. From equation A10:

$$\overline{H_{Jdx}} = \frac{1}{\sqrt{w^2 - b^2}} \frac{J_c dx i x^2 - b^2}{2\pi w - x}. \quad (53)$$

Trying to integrate over (b, a_1) again gives us singularities:

$$\overline{H_1(w)} = \frac{1}{\sqrt{w^2 - b^2}} \int_b^{a_1} \frac{i x^2 - b^2}{2\pi w - x} J_c dx. \quad (54)$$

We might want to try and add or subtract a function proportional to $1/\sqrt{w^2 - b^2}$, since this resembles complete screening, and will not give us penetration in the interval $(-b, b)$. This will not work because we lost an important symmetry in the second part of equation 54 is asymmetric ($f(-b) \neq f(b)$), whereas equations 38 and 45 were both symmetric ($f(b) = f(-b)$). To make the second part of 54 symmetric we can multiply by $(w + x)/(w + x)$:

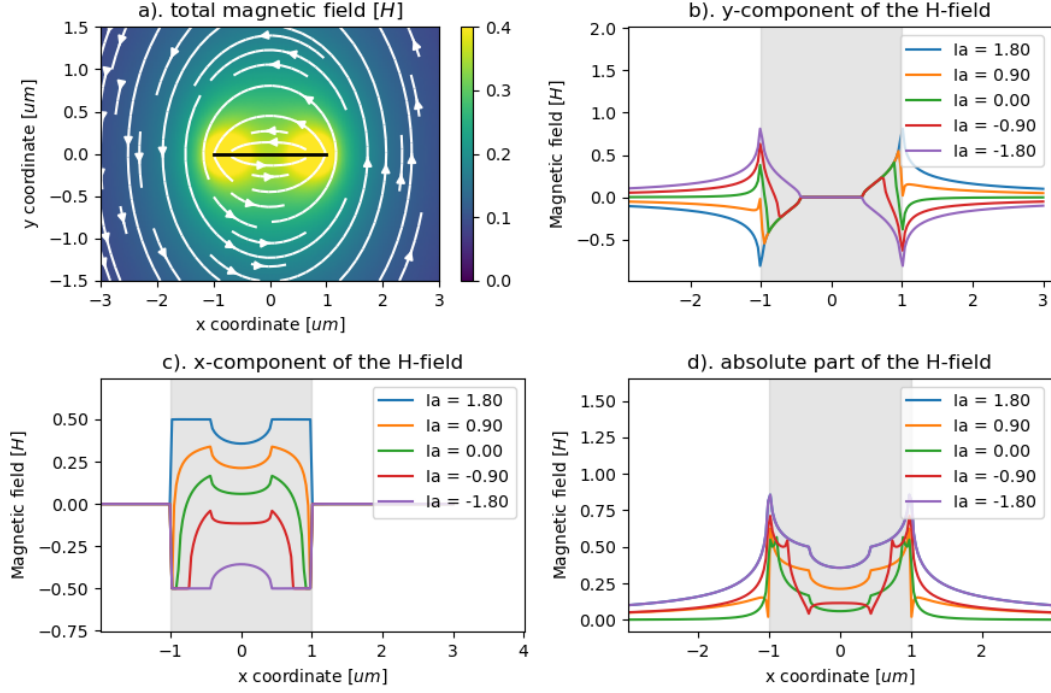


Figure 19: plot of 51 with $J_c = 1$, $I_0 = 1.8$, and varying I_a . The colormap in (a) is for the magnetic field on the intermediate step where $I_a=0$. The magnetic field in (b), (c), and (d) are taken very close to the real axis. (c) is also proportional to the current distribution in our sheet

$$\begin{aligned}
\overline{H_1(w)} &= \frac{1}{\sqrt{w^2 - b^2}} \int_b^{a_1} \frac{i}{2\pi} \frac{x^2 - b^2}{w - x} \frac{w + x}{w + x} J_c dx \\
&= \frac{1}{\sqrt{w^2 - b^2}} \frac{iJ_c}{2\pi} \int_b^{a_1} \frac{(w + x)(x^2 - b^2)}{w^2 - x^2} dx \\
&= \frac{w}{\sqrt{w^2 - b^2}} \frac{iJ_c}{2\pi} \int_b^{a_1} \frac{x^2 - b^2}{w^2 - x^2} dx \\
&\quad + \frac{1}{\sqrt{w^2 - b^2}} \frac{iJ_c}{2\pi} \int_b^{a_1} \frac{x(x^2 - b^2)}{w^2 - x^2} dx \\
&= \frac{w}{\sqrt{w^2 - b^2}} f_1(w) + \frac{1}{\sqrt{w^2 - b^2}} f_2(w)
\end{aligned} \tag{55}$$

Where we now recognize our equations for complete shielding of magnetic field, and current. Also since both f_1 and f_2 are symmetric ($f(b) = f(-b)$), we can create a solution free of singularities by:

$$H_h(w) = H_1 - \frac{w}{\sqrt{w^2 - b^2}} F_1 - \frac{1}{\sqrt{w^2 - b^2}} F_2$$

We call this solution H_h because it screens half of the sheet. With:

$$\begin{aligned}
F_1 &= f_1(\pm b), \\
F_2 &= f_2(\pm b).
\end{aligned}$$

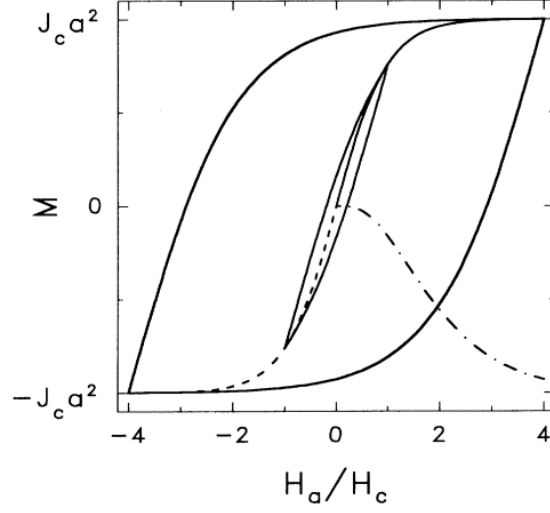


Figure 20: Magnetic Moment hysteresis curve taken from Brandt[3]. Two cycles of the magnetic moment after increasing the applied magnetic field from 0 to H_0 , to $-H_0$, and back to H_0 . the magnetic field starts at the 'virgin state' ($H_a = 0$, and $M = 0$, as it has just been cooled under zero-field to superconducting temperatures) and will initially cause the magnetic moment to increase as well. If you then decrease the magnetic field the magnetic moment will take the less steep curves back, and even end up having magnetic moment after being back at zero field (and even well below that). Then increasing the magnetic field again leaves you with the two cycles shown, these two cycles are for $H_0 = 1/4H_c$ and $H_0 = H_c$. The dash-dotted line is the remnant magnetic moment, and the dashed line is for decreasing magnetic field from the virgin state to $-H_c$

This gives:

$$\begin{aligned}
\overline{H_h(w), b, a_2} &= \frac{w}{\sqrt{w^2 - b^2}} \frac{iJ_c}{2\pi} \int_b^{a_1} (x^2 - b^2) \left[\frac{1}{w^2 - x^2} - \frac{1}{b^2 - x^2} \right] dx \\
&\quad + \frac{1}{\sqrt{w^2 - b^2}} \frac{iJ_c}{2\pi} \int_b^{a_1} x(x^2 - b^2) \left[\frac{1}{w^2 - x^2} - \frac{1}{b^2 - x^2} \right] dx \\
&= w\sqrt{w^2 - b^2} \frac{iJ_c}{2\pi} \int_b^{a_1} \frac{1}{(w^2 - x^2)\sqrt{x^2 - b^2}} dx \\
&\quad + \sqrt{w^2 - b^2} \frac{iJ_c}{2\pi} \int_b^{a_1} \frac{x}{(w^2 - x^2)\sqrt{x^2 - b^2}} dx \\
&= \sqrt{w^2 - b^2} \frac{iJ_c}{2\pi} \int_b^{a_1} \frac{x + w}{(w^2 - x^2)\sqrt{x^2 - b^2}} dx \\
&= \sqrt{w^2 - b^2} \frac{iJ_c}{2\pi} \int_b^{a_1} \frac{1}{(w - x)\sqrt{x^2 - b^2}} dx
\end{aligned} \tag{56}$$

Integrating into:

$$\overline{H_h(w, b, a_1)} = -\frac{J_c}{2\pi} \left[\tan^{-1} \left(\frac{b^2 - wa_1}{\sqrt{b^2 - w^2}\sqrt{a_1^2 - b^2}} \right) - \pi/2 \right] \tag{57}$$

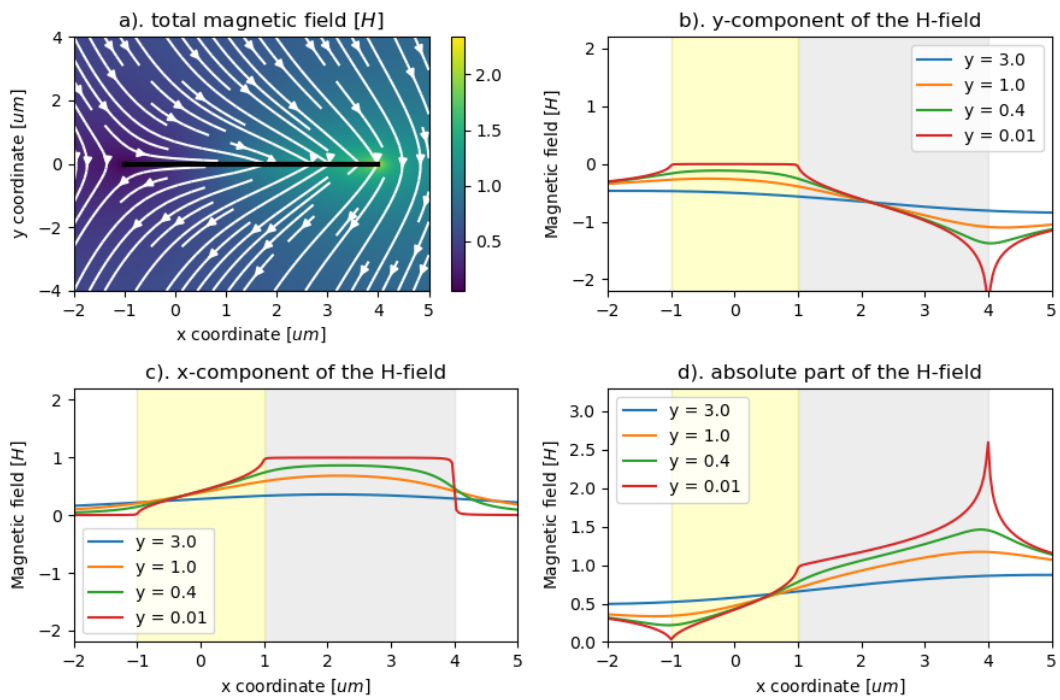


Figure 21: plot of 57 with $J_c = 2$, $a_1 = 4$, $b = 1$. The current density $H_0 = 1$, and varying H_a . The colormap in (a) is for the magnetic field on the intermediate step where $H_a=0$. The magnetic field in (b), (c), and (d) are taken very close to the real axis. (c) is also proportional to the current distribution in our sheet

This equation is visualized in figure 21 for $a_1 = 4$, $b = 1$, and $J_c = 1$.

If you increase an applied field H_0 , and a current I through our sheet at the same time, you get positive interference of the current on one side of the sheet and negative interference on the other side. This is because the current density is symmetric on the real axis for shielding magnetic field due to current (equation 48), and asymmetric for shielding of an applied magnetic field (42). Our previously derived equation is therefore also a description for increasing the applied magnetic field and current in the perfect balance such that the negatively interfering side perfectly cancels out. We call this perfect ratio between the applied magnetic field and current $r_p = \left(\frac{I}{H_0}\bigg|_{perfect}\right)$. If we increase the magnetic field and current, such that the ratio is higher than this perfect ratio, the magnetic field will have a higher impact on the distribution and thus the negatively interfering edge will get a current density of $-J_c$. This is therefore called a 'fieldlike' distribution. If we increase both but with a lower ratio, the current will become more dominant, and the negatively interfering side will get a density of $+J_c$. This is then called a 'currentlike' distribution. We can create these distributions by adding two 'halfsheet solutions'. Assume our sheet is located on the real axis in the interval $(-a_1, a_2)$ and is completely shielded from $(-b, b)$ center our axis around the shielded region and see. Then if we have a fieldlike situation we expect the current density to be J_c in $(-a_1, -b)$, $-J_c$ in (b, a_2) , and such that the magnetic field is perfectly shielded in $(-b, b)$. The solution can then be written as a superposition of equation 57 twice:

$$H_{\text{fieldlike}}(w, a_1, a_2, b) = H_h(-w, b, a_1) - H_h(w, b, a_2) \quad (58)$$

Which we visualize in figure 22 using $a_1 = 4$, $b = 1$, and $a_2 = 2$.

For currentlike increase of a sheet from $(-a_1, a_2)$ with shielded region $(-b, b)$, we get critical current density $+J_c$ at both intervals $(-a_1, -b)$ and (b, a_2) leading to:

$$H_{\text{currentlike}}(w, a_1, a_2, b) = H_h(-w, b, a_1) + H_h(w, b, a_1) \quad (59)$$

Which is visualized in figure 23. Using again $a_1 = 4$, $b = 1$, and $a_2 = 2$. Brandt[3] shows that for a 'half-sheet' solution the shielded magnetic field and bias current are:

$$\begin{aligned} H_h &= \frac{J_c}{2\pi} \cosh^{-1}(a_1/b), \\ I_h &= J_c \sqrt{a_1^2 - b^2}. \end{aligned} \quad (60)$$

To calculate the total magnetic field of equations 58 or 23 add both components their magnetic field and current, remembering that the magnetic field is asymmetric in the imaginary axis, and the current symmetric.

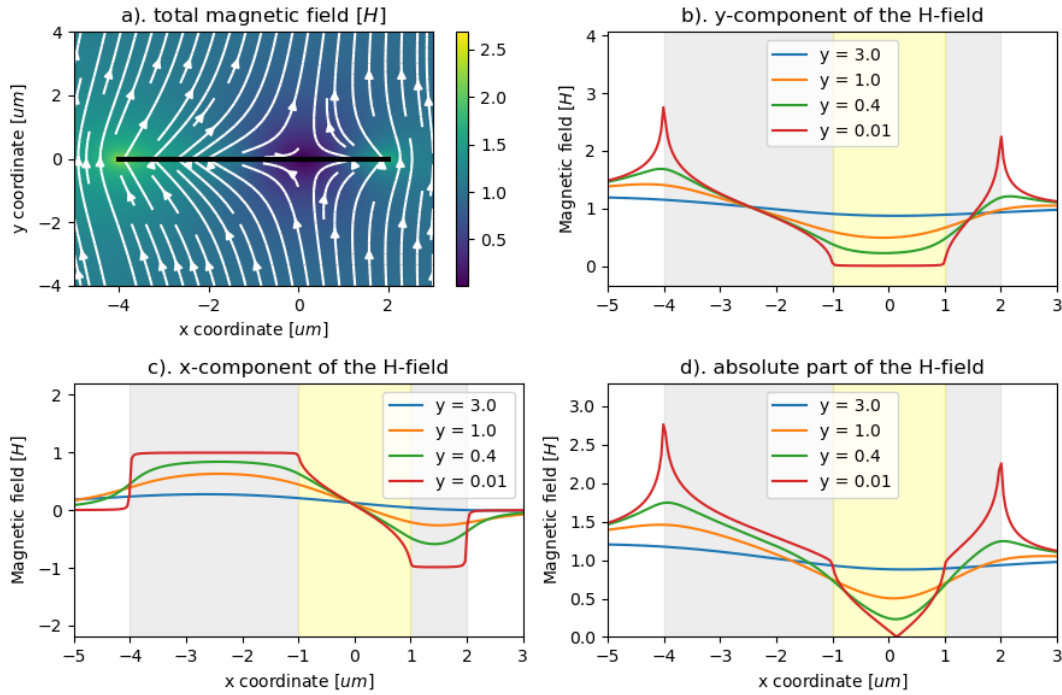


Figure 22: 'Fieldlike' behaviour after increasing both H and I . Equation 58 with $a_1 = 4$, $b = 1$, $a_2 = 2$. The yellow region shows the completely shielded regions of our sheet, and the grey areas are the parts where critical current is reached.

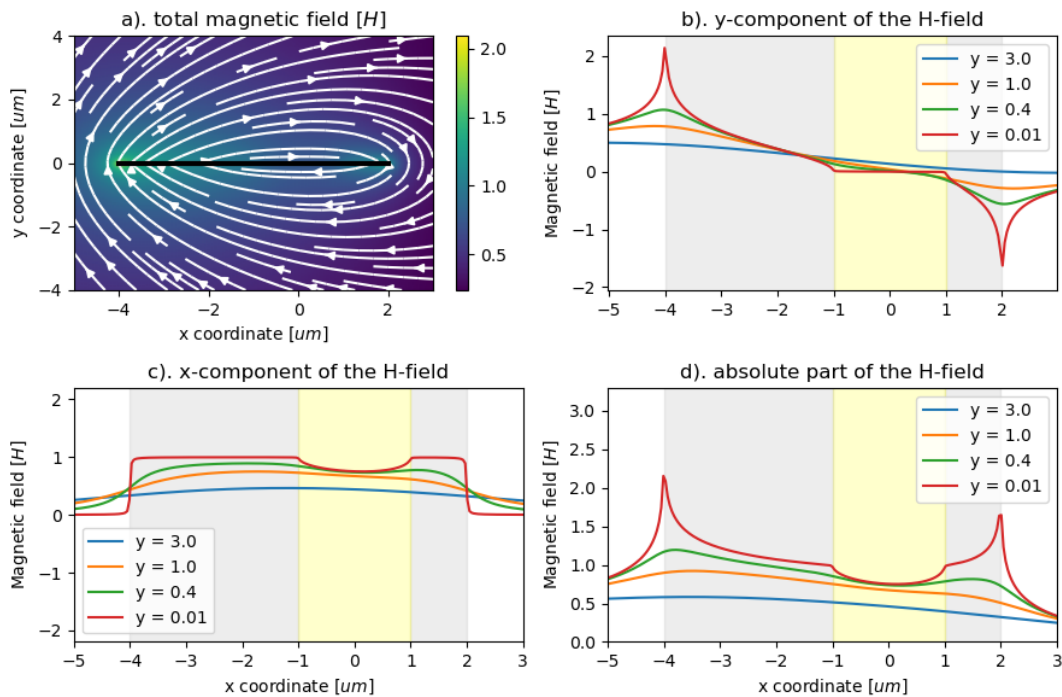


Figure 23: 'Currentlike' behaviour after increasing H and I simultaneously. Equation 23 with $a_1 = 4$, $b = 1$, and $a_2 = 2$. The yellow part is again the completely shielded part of the sheet.

4. Comparison with experimental results and discussion

Near the end of my thesis time frame, the Van der Sar lab started making measurements of the exact situations for which I was researching the equations. Here a diamond scanning probe with a single NV-centre (Nitrogen Vacancies) is used to accurately and non-invasively measure the magnetic field very close to a sample[16]. At first, we did not find good fits for our theorems. The results seemed to imply a certain 'offset field' passing through our superconductor without being screened at all. With an offset field and defining our shielded field as:

$$H_{shielded} = H_{applied} - H_{offset}, \quad (61)$$

we got very close fits as seen in figure 24. Here a measurement is shown for an applied field of $H_a = 5.5mT$ on the left, and the fitted parameters for a magnetic field sweep on the right.

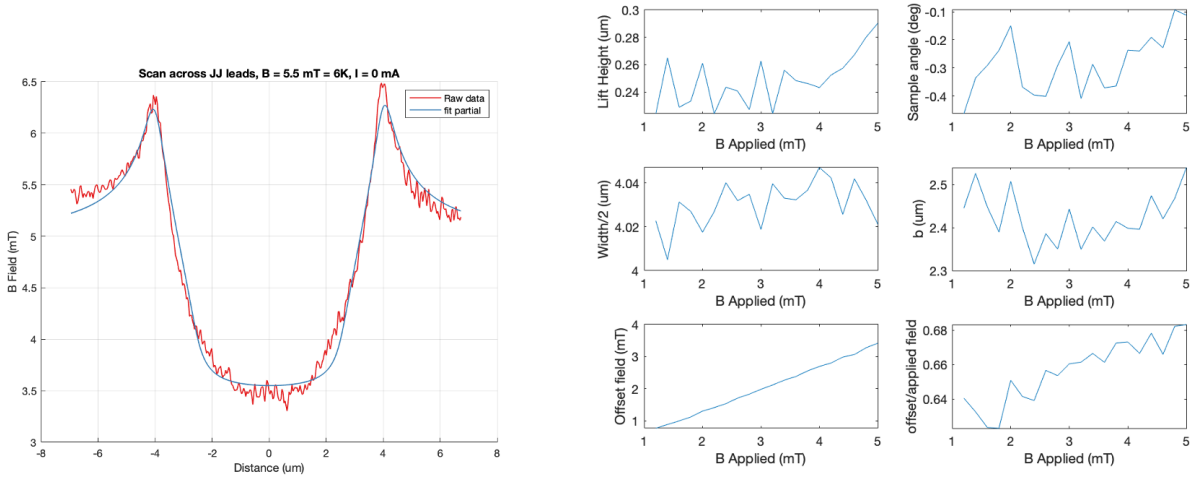


Figure 24: Measurements made and fitted by Dr. S. Kurdi and Ir. R. Mulder. Multiple measurements of our sheet have been done with applied magnetic fields increasing from $1mT$ to $5.5mT$. The situation for an applied magnetic field of $5.5mT$ is shown on the left. The fitted parameters of the sweep are shown on the right. The simulation is achieved by fitting equation 42, where w is based upon the x position, lift height, and angle. We fit the lift height of our NV-center from the sheet, and the angle of our sample (which we implemented due to the asymmetric field measured as seen by the two peaks), the half-width, which is equivalent to a in our equations. The completely screened part (b in our equations), and the offset field. Lastly, we also plotted the ratio of our offset field with the applied field.

The offset field is not explainable with our equations or theory, also it should be noted that b (which is the shielded region) seems to stay constant, whereas we expect an increase with field (equation 44). If we apply a reconstruction algorithm as explained in appendix B we see a reconstructed current distribution that does not completely seem to comply with our theoretic results (figure 25). It seems here as though the current distribution looks more similar to a linear distribution through the sheet than any of our results for shielding magnetic fields.

We are still in the process of improving and discovering new things about our setup. We currently have two leads in explaining the difference between theory and experimentation.

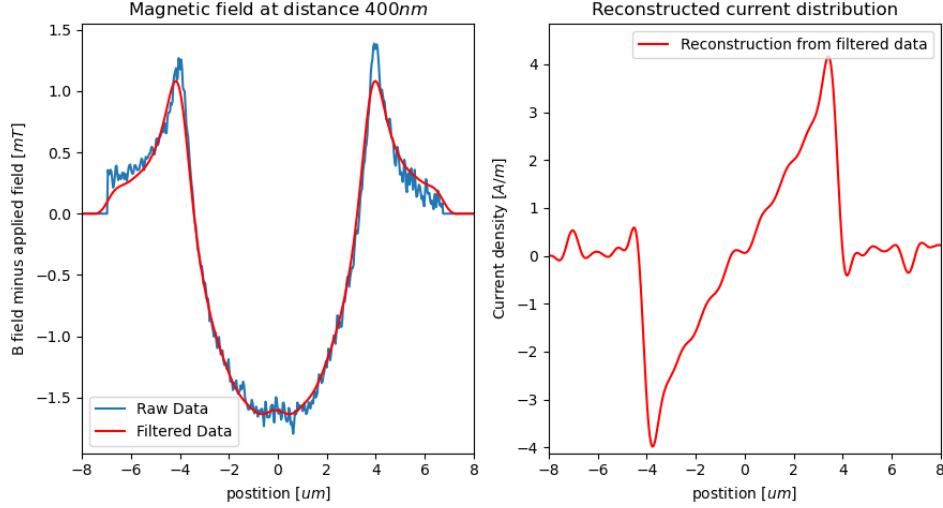


Figure 25: Current reconstruction from the data measured by Dr. S. Kurdi and Ir. R. Mulder a current reconstruction as explained in appendix B. Height = $.4\mu m$ is used to get the most realistic-looking current distribution. An artifact of our reconstruction method is the result of the lowpass filter. As seen the peaks seem to get smoothed out in the left figure, and we end up with lower frequencies on the right reconstruction seemingly showing current outside our sheet.

The first theory has to do with a later paper by Brandt[10], in which he revisits his calculations for superthin superconductors and takes the London penetration depth into account. This London penetration depth is a property of superconducting materials which dictates a penetration of magnetic field parallel to the superconductor[17]. This depth has been neglected throughout this thesis and the earlier works of Brandt and Norris. However, the London penetration depth for our material is around $200nm$, and our sheet dimensions are $8\mu m$ by $60nm$.

The second theory has to do with our setup. As stated before, we measure with an NV center. This center is aligned on a certain axis, which is the direction of the magnetic field we are sensitive to in our measurements. As preparation for measurements to come, the tips axis is mounted 45° in the y/z plane. Meaning that it is sensitive to magnetic field in the y direction (up and down in our graphs), and the z direction (into and out of the plane in our graphs). Therefore, the measurements are also sensitive to parasitic B fields in the z direction. Dr. S. Kurdi is currently looking into

There are two more papers I would like to discuss together. The first one is from Bobyl[18]. He measures the magnetic field around a thin sheet using magneto-optical imaging and gets plots of the reconstructed current density as shown in figure 26. For reconstruction, they use a similar method as we did (appendix B). These results are the closest I have been able to find to the Brandt equations/model. One approximation we have yet to discuss is the approximation for a constant critical current density J_c , whereas this is shown to be field-dependent. When J_c is made field-dependent ($J_c(B(x))$) equations 41 and 47 will have $J_c(B(x))$ in the integral and they would then not be integrable. Cun Xue[9] has tackled this problem numerically resulting in distributions where the edges (where the magnetic field is strongest) have the lowest critical current densities, which may explain the dips on the sides of figure 26a.[18]

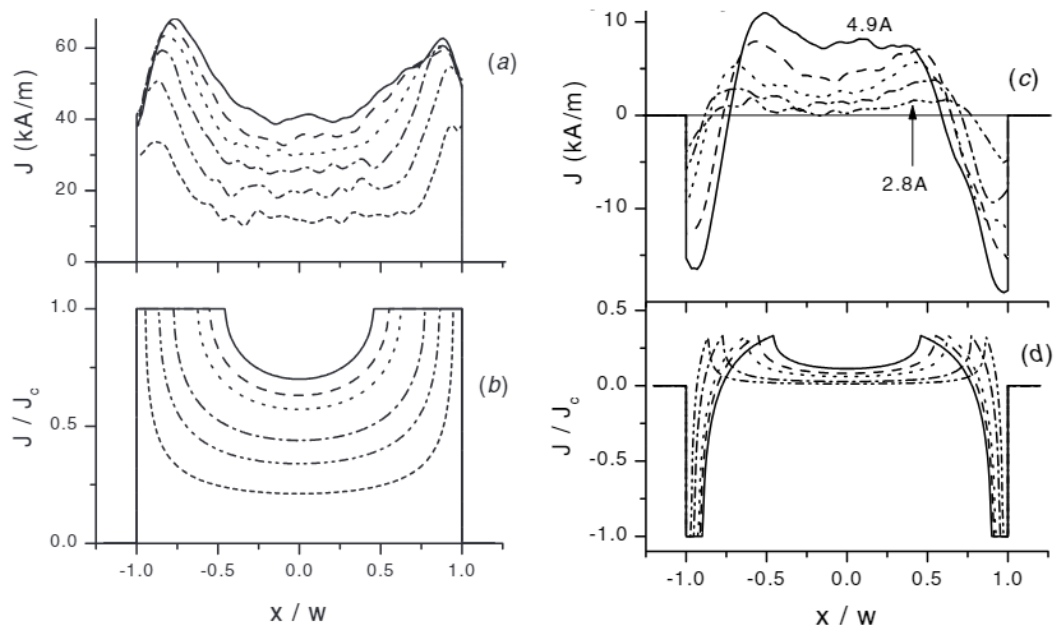


Figure 26: Measurement and analysis from Bobyl[18]. (a) shows current reconstruction after field measurements above the strip from $I = 1.8A$ to $I = 4.9A$, (b) shows theoretic current distributions using equation 48. (c) shows hysteresis after a pulse current is sent through the wires with pulse strength increasing from $I = 2,8A$ to $4,9A$. In (d) theoretical plots are made from equation 19 with $I_c = 5,5A$.

5. Conclusion

In this bachelor's thesis, we have extensively looked into the theory of calculating magnetic fields around superconductors using conformal mappings. These conformal mappings are used to satisfy the conditions that the superconductor screens magnetic flux, which is due to the Meissner effect. We first laid down some ground theorems on superconductors and conformal mappings, to help us in our applications.

In our applications, we looked at complete screening of an applied magnetic field, complete screening of a magnetic field due to a bias current, complete screening for thicker slabs of either applied magnetic field or magnetic field due to bias currents (which also gave us the tools to calculate the magnetic field around any symmetric polygonal shape). After complete shielding, we looked at methods for finite shielding first completed by Norris[1] and Brandt[2][3], which involve capping a current density J_c and shielding this magnetic field. Then, we looked at hysteresis; the results of alternating currents or magnetic fields on a superconductor. Lastly, we wrote the method of finitely screening a magnetic field combined of both an applied part and a part due to a bias current.

In the last section, we looked at the results of the Van der Sar lab low-temperature measurement setup, with measurements by Dr. S. Kurdi and Ir. R. Mulder. We discussed our models three shortcomings: neglecting the London penetration depth, having J_c be independent of the magnetic field and having a setup potentially sensitive to parasitic fields in the z direction. The first of these problems are taken into account in papers by Brandt[10] and Xue[9]. Also, measurements from Bobyl[18] were discussed.

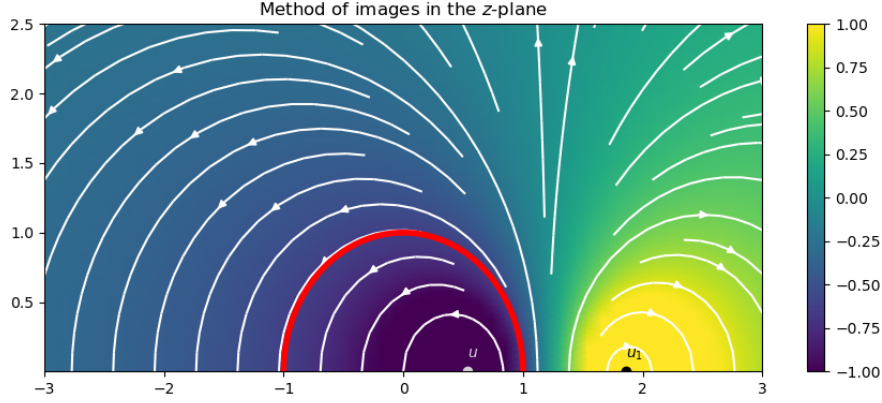


Figure 27: Problem for the method of images. Here we use the solution we will get at the end of this section to mirror a current filament u_1 with the virtual filament u' to have a parallel magnetic field around the circle C around the origin with $R = 1$. The colormap shows the complex part of our potential and the white arrows are the magnetic field lines of the two current filaments combined.

Appendix A Method of magneto-static images with circular boundary conditions

In this section, we will look at two current filaments going in opposite directions (into and out of our plane), and show that the magnetic field lines will point in circles. We will then show how to use this characteristic to mirror a current filament with another to obey boundary conditions, where a magnetic field is parallel to a circle at $(0, 0)$ with radius R . This would in itself be a solution to the magnetic field around a superconducting circular wire of radius R , when subjected to a small wire carrying I next to it. We will take it a step further, by mapping our circle with the parallel magnetic field to a sheet in the w -plane. Now the solution we get is how the magnetic field around a superconducting sheet would look when subjected to a wire with current I . This will later be used in our methods to calculate the magnetic field around a finitely shielding superconductor.

we look at the problem sketched in figure 27. We have a current filament at $z = u_1$, and a superconducting sphere around the origin with radius R . Now we see how we can place a 'virtual' current filament inside the superconducting cylinder at u' such that the magnetic field perpendicular around every point on the superconducting circle is zero.

Now consider two current filaments of strength I , and $-I$ (into, and out of the page) at u' and u_1 respectively. The complex potential then becomes the sum of the two (see equation 13):

$$\begin{aligned}
\mathcal{A} &= \frac{I}{2\pi} (\mathbf{Log}(z - u') - \mathbf{Log}(z - u_1)) i \\
&= \frac{I}{2\pi} \left(\mathbf{Log}(r' e^{i\theta'}) - \mathbf{Log}(r_1 e^{i\theta_1}) \right) i \\
&= \frac{I}{2\pi} \left(\log\left(\frac{r'}{r_1}\right) + i(\theta' - \theta_1) \right) i \\
&= \frac{I}{2\pi} \left(i \log\left(\frac{r'}{r_1}\right) - (\theta' - \theta_1) \right)
\end{aligned} \tag{A1}$$

Where $r' = |z - u'|$, $r_1 = |z - u_1|$, $\theta' = \arg(z - u')$, and $\theta_1 = \arg(z - u_1)$. Now taking $b = \text{constant}$, we get our magnetic field lines. We also write $z = a + bi$.

$$\begin{aligned}
c &= b(r, \theta) = \frac{I}{2\pi} \mathbf{Log} \frac{r'}{r_1} \\
\exp\left\{\frac{2\pi}{I} c\right\} &= \frac{r'}{r_1} = \frac{|z - u'|}{|z - u_1|} \\
\exp\left\{\frac{4\pi}{I} c\right\} &= \frac{|a + bi - u'|^2}{|a + bi - u_1|^2} = \frac{(a - u')^2 + b^2}{(a - u_1)^2 + b^2} \\
\exp\left\{\frac{4\pi}{I} c\right\} ((a - u_1)^2 + b^2) &= (a - u')^2 + b^2
\end{aligned}$$

We consider the exponential as constant (if I is also a steady current), assume $c > 0$, and can then substitute $\exp\left\{\frac{4\pi}{I} c\right\} = C > 1$. In doing so we get the general equation for a circle:

$$\begin{aligned}
0 &= -C((a - u_1)^2 + b^2) + (a - u')^2 + b^2 \\
&= (1 - C)(a^2 + b^2) + 2a(u_1 C - u') + u'^2 - C u_1^2 \\
0 &= a^2 + b^2 - 2a \frac{u' - u_1 C}{1 - C} + \frac{u'^2 - C u_1^2}{1 - C} \\
&= \left(a - \underbrace{\frac{u' - u_1 C}{1 - C}}_{\substack{\text{x-coordinate} \\ \text{of center of circle}}} \right)^2 + b^2 - \underbrace{\left(\frac{u' - u_1 C}{1 - C} \right)^2 + \frac{u'^2 - C u_1^2}{1 - C}}_{\text{radius of circle squared}}
\end{aligned} \tag{A2}$$

In our symmetry we want the circle to be centered at $(0, 0)$, and have radius R , this leads to:

$$u' - u_1 C = 0 \tag{A3}$$

$$-\left(\underbrace{\frac{u' - u_1 C}{1 - C}}_{\text{zero by eq. A3}} \right)^2 + \frac{u'^2 - C u_1^2}{1 - C} = -R^2 \tag{A4}$$

We solve these equations for u' by substituting $C = u'/u_1$ (a direct consequence of equation A3) into equation A4 (In our method of images problem, we are given a u_1 , and R). Then solving gives us:

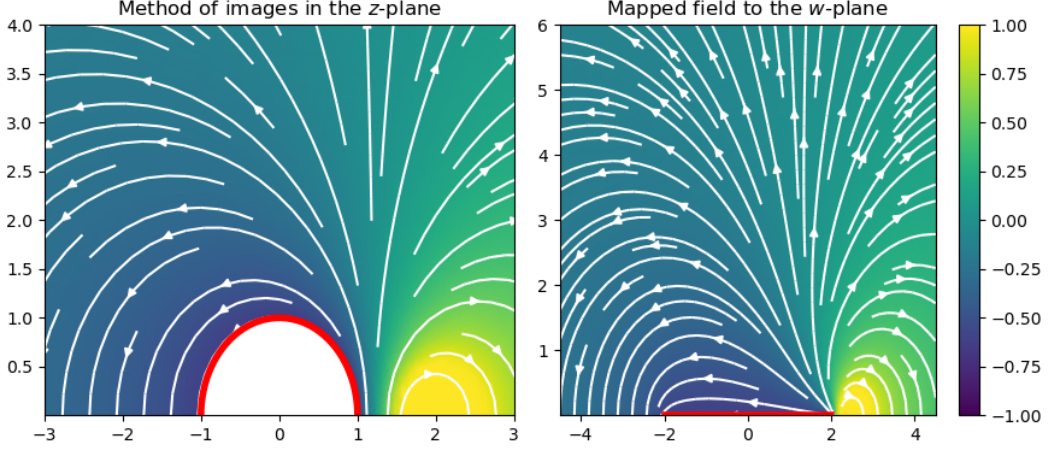


Figure 28: Method of mirroring of a single source in the z -plane, where we map the magnetic field to the w -plane using a Joukowski mapping.

$$u' = \frac{1}{2} \left(u_1 + \frac{R^2}{u_1} \right) \pm \frac{1}{2} \sqrt{\left(u_1 + \frac{R^2}{u_1} \right)^2 - (2R)^2} \quad (\text{A5})$$

Here we discard the *plus*-solution since it would place our negative current filament directly on the positive current filament, resulting in a trivial solution where the magnetic field is zero everywhere. Not only is it trivial, but it also places a charge on our domain, which cannot happen in the method of images.

In principle, we are done at this point and know how to mirror a charge such that the prerequisite boundary conditions are met. However, it is interesting to note that a form of the Joukowski mapping is present twice in the equation (equation 15). So we can write $w_1 = u_1 + \frac{R^2}{u_1}$. If we want to shield the unit circle we get $R = 1$, and we know the inverse of u_1 coming from w_1 :

$$u' = \frac{1}{2} \left(w_1 - \sqrt{w_1^2 - 4} \right) \quad (\text{A6})$$

$$u_1 = \frac{1}{2} \left(w_1 + \sqrt{w_1^2 - 4} \right) \quad (\text{A7})$$

Because the Joukowski mapping maps the upper unit circle to the real axis between $(-2, 2)$, we have found a way to also shield a sheet from a current filament in the plane of the sheet. This is shown in figure 28.

If we look at a point in the z -plane and remember its correlation to the w -plane:

$$z = \frac{1}{2} \left(w + \sqrt{w^2 - 4} \right) \quad (\text{A8})$$

We can find the magnetic field in the z -plane as:

$$\begin{aligned}
\overline{\tilde{H}(z)} &= \frac{d\mathcal{A}}{dz} \\
&= \frac{Ii}{2\pi} \left(\frac{1}{z - u_1} - \frac{1}{z - u'} \right) \\
&= \frac{Ii}{2\pi} \left(\frac{u_1 - u'}{(z - u')(z - u_1)} \right)
\end{aligned}$$

Where we can show from equation A6 and A7 that $u_1 - u' = \sqrt{w_1^2 - 2}$ and $(z - u')(z - u_1) = z(w - w_1)$, resulting in:

$$\overline{\tilde{H}(z)} = \frac{Ii}{2\pi} \left(\frac{\sqrt{w_1^2 - 4}}{z(w - w_1)} \right) \quad (\text{A9})$$

Before plugging everything in 9, note one more niceness of the equations:

$$\begin{aligned}
z \frac{df}{dz} &= z \left(1 - \frac{1}{z^2} \right) = z - \frac{1}{z} \\
&= \frac{1}{2} \left(w + \sqrt{w^2 - 4} \right) - \frac{1}{\frac{1}{2} \left(w + \sqrt{w^2 - 4} \right)} \\
&= \frac{w^2 + w\sqrt{w^2 - 4} - 4}{\left(w + \sqrt{w^2 - 4} \right)} = \sqrt{w^2 - 4}
\end{aligned}$$

Now according to 9:

$$\begin{aligned}
\overline{H(w)} &= \frac{\overline{\tilde{H}(z(w))}}{f'} \\
&= \frac{Ii}{2\pi} \frac{\sqrt{w_1^2 - 4}}{\sqrt{w^2 - 4}(w - w_1)}
\end{aligned}$$

Now to go one step further we want our sheet to range from $(-b, b)$, instead of $(-2, 2)$. We can simply do this by mapping $(w, w_1, I) \rightarrow (2w/b, 2w_1/b, 2I/b)$ giving:

$$H(w) = \frac{Ii}{2\pi} \frac{\sqrt{w_1^2 - b^2}}{\sqrt{w^2 - b^2}(w - w_1)} \quad (\text{A10})$$

This is an extremely important result since it shows how to shield any current filament at w_1 from penetrating a superconducting sheet of width $2b$. When we start calculations on finite screening, we assume a certain critical current density at the edges, which we can then screen through this equation.

I have also slightly altered the equation such that current filaments above the superconductor are also possible. Then I placed two sources at $z_1 = 2.3 + i$ and $z_2 = -2.1 + 3j$, and put that plot on the cover of my thesis. This plot is thus the magnetic field above a superconductor subject two wires carrying current.

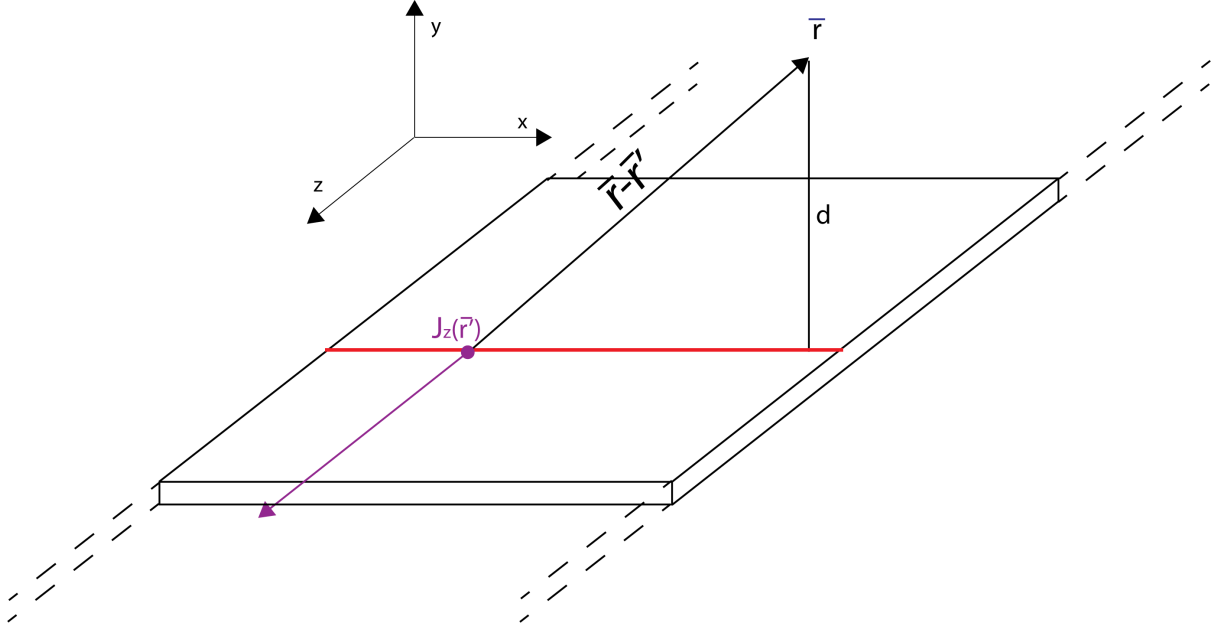


Figure 29: Sketch for the magnetic field above a current carrying sheet. The sheet holds a current distribution pointed in the z -direction denoted by $J_z(\bar{r}')$, with $\bar{r}' = (x', 0, 0)$. This current density is assumed constant over all of z . We look at the magnetic field of a point \bar{r} a distance d above the sheet $\bar{r} = (x, d, 0)$

Appendix B Current reconstruction from magnetic field

The measurement will give us $H_y(x)$ at a distance d above the strip as a result of our current distribution in the strip (figure 29). Our previous analysis gives us the magnetic field due to a predetermined current distribution, which we will compare with the measured field. However, it is also very valuable to compare our measured and theorized current distributions. This gives us the inverse problem of calculating the current distribution $J(\mathbf{r}')$ from the magnetic field $H_y(\mathbf{r})$. A solution to this $1D$ problem is given by Zuber [19] and a solution to the $2D$ problem by Bradley J. Roth [20]. We will follow the former until the low-pass filters, where the latter seems to give us a better solution.

For the inverse problem, we make a few assumptions. We first assume that the current is only dependent on x , and only has a z component. Now through symmetry, we can conclude that the \mathbf{H} field has no z -component and is only dependent on its x -coordinate. These result in the following expressions for \mathbf{J} , and \mathbf{H} :

$$\begin{aligned} \mathbf{J}(\mathbf{r}') &= \begin{bmatrix} 0 \\ 0 \\ J_z(x') \end{bmatrix} \\ \mathbf{H}(\mathbf{r}) &= \begin{bmatrix} H_x(x, y) \\ H_y(x, y) \\ 0 \end{bmatrix} \end{aligned} \quad (\text{A11})$$

If we look at the resulting magnetic field from an infinitesimally small slit (thickness dx' , total current $J(x')dx'$) of the superconducting sheet we can apply the Biot-Savart law for moving

charge and integrate this over y from $-\infty$ to ∞ . This is done in many electrostatic textbooks (eg. Griffith's [14]) and gives us:

$$\mathbf{H}(\mathbf{r}; \mathbf{r}') = 2\pi \frac{\mathbf{J}(\mathbf{r}') \times (\mathbf{r}' - \mathbf{r})}{|\mathbf{r}' - \mathbf{r}|^2} dx' \quad (\text{A12})$$

Here $\mathbf{H}(\mathbf{r}; \mathbf{r}')$ is the magnetic field due to the current $\mathbf{J}(x')dx$. Integrating equation A12 over x' and substituting equation A11 into the cross-product (with $(\mathbf{r}' - \mathbf{r}) = (x' - x, -d, 0)$) results in:

$$\begin{aligned} \mathbf{H}(x, y = d) &= \frac{1}{2\pi} \int_{-\infty}^{\infty} \frac{J_x(x')}{(x' - x)^2 + d^2} \begin{bmatrix} -d \\ (x' - x) \\ 0 \end{bmatrix} dx' \\ \implies H_y(x, y = d) &= \frac{1}{2\pi} \int_{-\infty}^{\infty} J_x(x') \frac{(x' - x)}{(x' - x)^2 + d^2} dx' \\ &= (J * G)(x) \end{aligned} \quad (\text{A13})$$

Where

$$G(x, x') = G(x - x') = \frac{1}{2\pi} \frac{(x' - x)}{(x' - x)^2 + d^2} \quad (\text{A14})$$

Here G is called the Kernel (K) by Zuber [19] and a Green's function by Roth [20]. Equation A13 is a way of calculating the magnetic field from the current distribution. To inverse the equation we take advantage of the convolution, which becomes a multiplication in the Fourier domain. Translating equation A13 to Fourier space gives us:

$$\begin{aligned} h_y(k) &= j(k)g(k) \\ \implies j(k) &= \frac{g(k)}{h_y(k)} \end{aligned}$$

Where h_y , j , and g are the Fourier transforms of H_y , J , and G respectively. Now J becomes:

$$J(x) = \mathcal{F}^{-1} \left[\frac{g}{h_y}(k) \right] (x) \quad (\text{A15})$$

It is shown in appendix E that $g(k)$ can be evaluated:

$$g(k) = -\frac{i}{2} \text{sgn}(k) e^{-d|k|} \quad (\text{A16})$$

This would be the end of our problem, if not for noise. The higher frequencies blow up in equation A16, and noise is translated to high frequencies in the Fourier domain. We filter out our higher frequencies using a Hanning window [21] in Fourier space:

$$w(k) = \begin{cases} 0.5 \left[1 + \cos \left(\frac{\pi k}{k_{max}} \right) \right], & \text{if } |k| < k_{max} \\ 0, & \text{otherwise} \end{cases} \quad (\text{A17})$$

This is the equation where Zuber [19] and Roth [20] split ways. Zuber uses the simple low-pass filter:

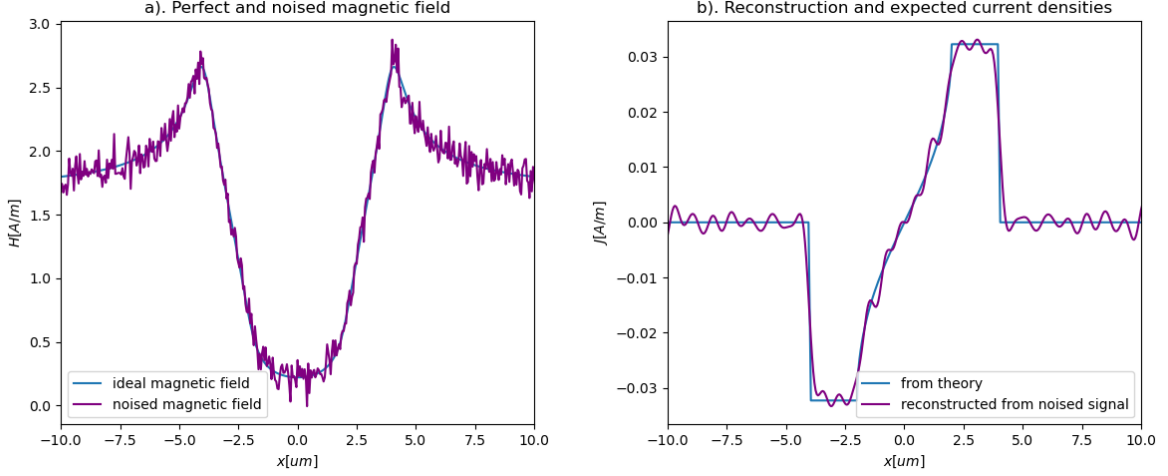


Figure 30: Reconstruction of current density using equation A18. In (a) we plot the magnetic field according to equation 42 at a distance $.4um$ above the superconductor twice, where we have added noise to one of the two. (b) contains the current density affiliated with the magnetic field from (a) according to equations 42 and A21, and the current distribution reconstruction from the noised magnetic field according to equation A18, with $d = .4um$.

$$w_2(k) = \begin{cases} 1, & \text{if } |k| < k_{max} \\ 0, & \text{otherwise} \end{cases}$$

Which he then evaluates to get a nice direct description of $J(x)$. In our case with the Hanning window, we get for our current reconstruction:

$$J(x) = \mathcal{F}^{-1} \left[\frac{gw}{b_y}(k) \right] (x) \quad (\text{A18})$$

Which works better from trial and error experience. Figure 30 shows how close this approximation gets when met with noise. Here we have used our theoretic results for finite shielding of a magnetic field (equation 42). You see that a frequency has been introduced to our inverse, this is due to the deleted higher frequencies in the Fourier domain.

Appendix C Proportionality of magnetic field to current distribution

In this section, we explain show the proportionality of the magnetic field close to the superconductor with the current density inside it. We prove this using Ampere's law:

$$\oint_C H dL = I_{encl} \quad (\text{A19})$$

First, we show some characteristics of our magnetic field. If you look at figure 31a we can see the magnetic field caused by a current filament $I = J dx$ on our superconducting sheet. Two

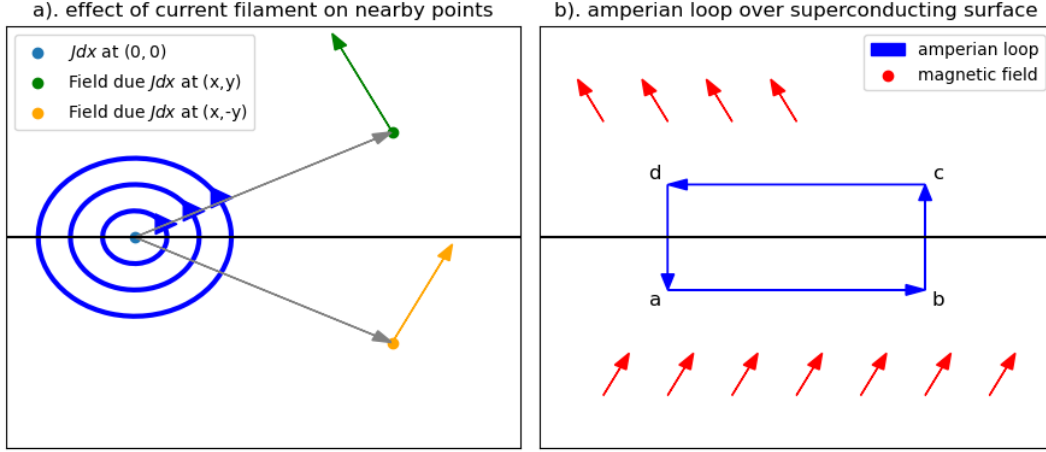


Figure 31: (a). shows the magnetic field at two mirrored points due to a current filament $I = Jdx$. (b). shows the Amperian loop we use to show equation A21.

points have been chosen close to the superconductor to compare. Knowing $H \propto I \times r$, we can write:

$$\begin{aligned}
 H(x, y) &\propto \begin{bmatrix} -y \\ x \\ 0 \end{bmatrix} \\
 H(x, -y) &\propto \begin{bmatrix} y \\ x \\ 0 \end{bmatrix} \\
 \implies H_y(x, y) &= H_y(x, -y) \\
 \wedge H_x(x, y) &= -H_x(x, -y)
 \end{aligned} \tag{A20}$$

Which shows a symmetry we often use to mirror our results to the negative real plane. If you look at $y = 0$ something interesting happens: the magnetic field is continuous in the y -direction, and discontinuous in the x -direction. This is also shown in figure 31a, since the x -component of the field in the upper half is negative, and the x -component in the lower half is positive, whilst the y -components keep the same sign. We now look at the Amperian loop in figure 31b

We also know that the magnetic field is continuous everywhere there is no current because it then follows equation 3. Now applying Ampere's law (equation A19) to figure 31b, we see that the integrals from $b \rightarrow c$ and $d \rightarrow a$ cancel each other for a small enough loop due to the continuity of the y -component of the field. The integral from $a \rightarrow b$ and $c \rightarrow d$ yields $2 \int_c^d H(z) dz$ (due to the negative symmetry they are equal). Also $I_{encl} = \int J dx$ through the part of the superconductor enclosed. Because both J and H are continuous on these domains we can take the limit and get:

$$J(x) = 2 \lim_{b \downarrow 0} H_x(x + bi) \tag{A21}$$

This is always for the H field due to the current in the sheet itself. In some examples, we apply an external H -field in the y -direction, but it is clear that this does not affect H_x nor I_{encl} , and

therefore our equation still holds. If the applied magnetic field has an x -component you would lose $H_x(x, y) = -H_x(x, -y)$ and have to be careful again.

Appendix D Magnetic field around normal conducting sheet with applied current

In this appendix, we look at the magnetic field expected from a normal conductor carrying a current I . The resistance per area in a normal conductor increases with the current distribution. Current follows the path of least resistance, and therefore we would expect the current distribution to be uniform. The complex magnetic potential of a current filament is given by equation 13. Now we consider the current-carrying sheet as an integral of infinitesimally small current filaments Jdx , where the uniform current density implies $J = I/(2a)$ everywhere on the sheet, where a is the half-width of the sheet (and therefore $2a$ the full width). This integral gives:

$$\begin{aligned} \mathcal{A}(z) &= \int_{-a}^a \frac{J}{2\pi} i \text{Log}(z-x) dx \\ &= -\frac{Ii}{4\pi} \frac{1}{z-x} \Big|_{x=-a}^a \\ &= \frac{Ii}{4\pi} \left(\frac{1}{z+a} - \frac{1}{z-a} \right) \end{aligned}$$

Then by equation 8:

$$\begin{aligned} \overline{H(z)} &= \frac{Ii}{4a\pi} \frac{d}{dz} \left(\frac{1}{z+a} - \frac{1}{z-a} \right) \\ &= \frac{Ii}{4a\pi} \text{Log} \left(\frac{z-a}{z+a} \right) \\ \overline{H(z)} &= \frac{Ii}{4a\pi} \text{Log} \left(\frac{z-a}{z+a} \right) \end{aligned} \tag{A22}$$

Which gives us the desired results for our magnetic field around the sheet. This equation is visualized in figure 10.

Appendix E code

Code used for visualizing our conformal mappings:

For our visualization of our results I wrote a general script, in which only the $h(w)$ function needs be added from our theoretical results:

```
# -*- coding: utf-8 -*-
"""
@author: TjipkeH
"""
```



```

from matplotlib import pyplot as plt
import numpy as np
import scipy

#plotting parameters.
#plotlim is limits of field plots
#m is limit of colorbar (necessary because it explodes around edges of
                                superconductor)

plotlim = [-3,3]
xdomain = [-7,7]
ydomain = [-2,2]
mapsteps = 600
m = 2

#ENTER PARAMETERS FOR YOUR FUNCTION HERE

#ENTER THE FUNCTION H HERE
def h(w) :
    return

#superconducting bar
t = np.linspace(0,2*np.pi,97)
curves = []
curves.append(np.linspace(-width,width,3))

#lines where we want to calculate the magnetic field
wt = np.linspace(xdomain[0],xdomain[1],211)
wcurves = []
wcurves.append(3j+wt)
wcurves.append(1*1j+wt)
wcurves.append(.4*1j+wt)
wcurves.append(.01j+wt)

xmap = np.linspace(xdomain[0],xdomain[1],mapsteps)
ymap = np.linspace(ydomain[0],ydomain[1],mapsteps)
Xmap, Ymap = np.meshgrid(xmap,ymap)
A = Xmap+(1j*Ymap)

#calculating our potential and H-field in original coordinates
TransformedH = np.conjugate(honw(A))

fig, ax = plt.subplots(2,2, figsize=[9,6])

#draw the w-grid and pretty colormaps
a = ax[0][0].pcolormesh(np.real(A), np.imag(A), np.abs(TransformedH), shading
                        ='gouraud', cmap='viridis', vmin=0,
                        vmax=m)
ax[0][0].streamplot(np.real(A), np.imag(A), np.real(TransformedH), np.imag(
                    TransformedH), density=.8, linewidth=
                    None, color='white')

fig.colorbar(a, ax= ax[0][0])

#name the axis and plots

```

```

ax[0][0].set(title = 'a). total magnetic field [ $H/H_0$ ]',
            xlabel = 'x coordinate[ $\mu\text{m}$ ]',
            ylabel = 'y coordinate[ $\mu\text{m}$ '])
ax[1][0].set(xlabel = 'x coordinate[ $\mu\text{m}$ ]',
            ylabel='Magnetic field [ $H/H_0$ ]',
            title = 'c). x-component of the H-field')
ax[0][1].set(xlabel='',
            ylabel='Magnetic field [ $H/H_0$ ]',
            title = 'b). y-component of the H-field')
ax[1][1].set(xlabel = 'x coordinate[ $\mu\text{m}$ ]',
            ylabel='Magnetic field [ $H/H_0$ ]',
            title = 'd). absolute part of the H-field')

for wcurve in (wcurves):
    ax[0][0].plot(np.real(wcurve), np.imag(wcurve))
    B = np.conjugate(honw(wcurve))
    ax[1][0].plot(np.real(wcurve), np.real(B), label=('y = '+str(np.imag(
        wcurve[0])))
    ax[0][1].plot(np.real(wcurve), np.imag(B), label=('y = '+str(np.imag(
        wcurve[0])))
    ax[1][1].plot(np.real(wcurve), np.abs(B), label=('y = '+str(np.imag(
        wcurve[0])))

for y in (curves):
    ax[0][0].plot(np.real(y), np.imag(y), color='black', linewidth=3)
    break

ax[1][0].fill_between([-width,width], [20,20], [-20,-20], alpha=0.2, color='
    grey')
ax[0][1].fill_between([-width,width], [20,20], [-20,-20], alpha=0.2, color='
    grey')
ax[1][1].fill_between([-width,width], [20,20], [-20,-20], alpha=0.2, color='
    grey')

ax[1][0].set_ylim(plotlim)
ax[0][1].set_ylim(plotlim)
ax[1][1].set_ylim([0,1.5*plotlim[1]])
ax[1][0].set_xlim(xdomain)
ax[0][1].set_xlim(xdomain)
ax[1][1].set_xlim(xdomain)

ax[0][0].set_ylim(ydomain)
ax[0][0].set_xlim(xdomain)

ax[1][0].legend()
ax[0][1].legend()
ax[1][1].legend()

# set the spacing between subplots
fig.tight_layout()
plt.show()

```

For perfect screening of applied magnetic field in a thin superconductor we use equation 25. Note that the equation is only defined on the upper complex plane, thus we use mirroring of the equation to get a solution in the lower plane:

```

#applied field and width of superconductor
H0=1
width=4

#h
def honw(w) :
    w2 = w/width
    temp = 1j*w2/(sq(w2**2-1))*H0
    temp = np.where(np.imag(w2)>0,-temp,temp)
    return temp

```

For perfect screening of a magnetic field due to bias currents in a thin superconductor, we use equation 29. Here we define a square root function over a different branch cut:

```

#applied current and width of superconductor
width = 3
I = 1

#h
def honw(z) :
    temp = I/(2*np.pi*np.sqrt(-(z)**2+width**2))
    temp = np.where(np.imag(z)<0,-temp,temp)
    return temp

def sq(z) :
    return 1j*((-z)**.5)

```

For partial screening of applied magnetic field in a thin superconductor we use equation 42. Here the tangent is also taken over a different branch cut:

```

#applied field and width of superconductor
#H0=1
width=4
Hshielded = 1
b = 2

limit = np.abs((np.arctan((width)/(1j*np.sqrt(width**2-b**2)))-np.pi/2))
#h
def honw(z) :
    temp = Hshielded/limit*(np.arctan((width*np.sqrt(b**2-z**2))/(z*np.sqrt(
        width**2-b**2)))-np.pi/2)
    temp = np.where(np.real(z) < 0, temp+np.pi*Hshielded/limit, temp)
    temp = np.where(np.imag(z)>0,temp,-temp)
    return temp

#functions required for other functions
def sq(z) :
    return 1j*((-z)**.5)

```

For partial screening of a magnetic field due to bias currents in a thin superconductor, we use equation 48:

```

#applied current and width of superconductor
width=4
b = 2+0j

```

```

I = 1

#h
def honw(z):
    Jc = I/(2*(width**2-b**2)**.5)
    temp = Jc/(np.pi)*np.arctan(np.sqrt(width**2-b**2)/np.sqrt(b**2-z**2))
    temp = np.where(np.imag(z)<0,-temp,temp)
    return temp

```

For an alternating magnetic field, we implement equation 50:

```

#variables
Jc = 1.5
H0 = 1
Ha = 0
w= 1+0j

Hc = Jc/np.pi

def h(z):
    if (Ha==H0):
        return Hd(z,H0,Jc)
    temp = Hd(z,H0,Jc)-Hd(z,H0-Ha,2*Jc)
    temp = np.where(np.imag(z)>0,temp,-temp)
    return temp

def Hd(z, Ha, Jc):
    Hc1 = Jc/np.pi
    b = w/np.cosh(Ha/Hc1)
    limit = np.abs((np.arctan((w)/(1j*np.sqrt(w**2-b**2)))-np.pi/2))
    temp = -Ha/limit*(np.arctan((w*np.sqrt(b**2-z**2))/(z*np.sqrt(w**2-b**2)))-np.pi/2)

    if np.real(z)<0:
        return temp-np.pi*Ha/limit
    return temp

```

For an alternating current, we implement equation 51:

```

Jc = 1
I0 = 1.8
Ia = 0
w= 1+0j
Hc = Jc/np.pi

def h(z):
    if (Ia==I0):
        return Hd(z,I0,Jc)
    return Hd(z,I0,Jc)-Hd(z,I0-Ia,2*Jc)

def Hd(z, I, Jc):
    Imax = Jc*2*np.real(w)
    b = w*(1-I**2/Imax**2)**.5
    temp = -Jc*1j/np.pi*np.arctanh(np.sqrt(b**2-w**2)/np.sqrt(b**2-z**2))
    temp = np.where(np.imag(z)>=0,temp,-temp)
    return temp

```

For a magnetic field due to a combination of bias currents and applied parts, we use equations 58 and 59:

```

b = 1+0j
a1 = 2+0j
a2 = 4+0j
Jc = 2+0j
Hc = Jc/np.pi
fieldlike = False
xdomain = [-np.real(a1)-1, np.real(a2)+1]

def h(z):
    z2 = np.conjugate(z)
    temp = np.where(np.imag(z)>0, Hhalf(z, Jc),
                    -np.conjugate(Hhalf(z2, Jc)))
    return temp

def Hhalf(z, Jc):
    def temp(z, a):
        return -Jc/(2*np.pi) * (np.arctan((b**2-z*a)/(np.sqrt(b**2-z**2)*np.
                                             sqrt(a**2-b**2))))-np.pi/2)
    if fieldlike:
        return -temp(z, a2)+temp(-z, a1)
    return temp(z, a2)+temp(-z, a1)

def Hcur(z, a, b, Jc):
    return -Jc*1j/np.pi*np.arctanh(np.sqrt(b**2-a**2)/np.sqrt(b**2-z**2))

def Hmag(z, a, b, Jc):
    temp = -Hc*(np.arctan((a*np.sqrt(b**2-z**2))/(z*np.sqrt(a**2-b**2)))-np.
                .pi/2)
    temp = np.where(np.real(z)<0, temp-np.pi*Hc, temp)
    return -temp

```

For a thick slab we first have to define a numerical inverse algorithm, a complex integration algorithm, and an application for equation 9:

```

from scipy.integrate import quad
from scipy import optimize

def h(w):
    return honz(inverseoff(g, gpr, w, w))
def honz(z):
    return np.conjugate(potder(z)/gpr(z))

def integ(f, z):
    a = np.real(z)
    b = np.imag(z)
    def realreal(re):
        return np.real(f(re+yfly*1j))
    def realim(re):
        return np.imag(f(re+yfly*1j))
    def imreal(im):
        return np.real(f(a+1j*im))
    def imim(im):
        return np.imag(f(a+1j*im))

```

```

repa = quad(realreal,0,a)[0]+1j*quad(realim,0,a)[0]#lambda x: expint(3,
                                     x)
impa = quad(imreal,yfly,b)[0]+1j*quad(imim,yfly,b)[0]
return repa+1j*impa

def inverseoff(f, fpr, z0,zw):
    def g2(z):
        return g(z)-zw
    test = optimize.newton(g2, 2+.0001j, fprime=fpr)
    return test

def gin(z):
    if np.imag(z)<0:
        return np.conjugate(inverseoff(g,gpr,np.conjugate(z),np.conjugate(z)))
    return inverseoff(g,gpr,z,z)

```

Which for infinite screening of a magnetic field becomes:

```

#potential, its derivative, and a function for h directly
def pot(z):
    return H0*z
def potder(z):
    return H0

#mapping
def g(z):
    if np.imag(z)<0:
        return np.conjugate(g(np.conjugate(z)))
    return integ(fpr,(z))-1j*offset#sq(z**2-1)
def gin(z):
    if np.imag(z)<0:
        return np.conjugate(inverseoff(g,gpr,np.conjugate(z),np.conjugate(z)))
    return inverseoff(g,gpr,z,z)
def sq(z):
    return 1j*((-z)**.5)
def gpr(t):
    return (sq(-t**2+a2**2))/(sq(-t**2+4))

```

And for our bias current case:

```

#potential, and its derivative:
def pot(z):
    return 1j*Ibi*np.log(z)
def potder(z):
    return 1j*Ibi/z

def sq(z):
    return 1j*((-z)**.5)

#mapping
def g(z):
    return integ(fpr,jouk(z))-1j*offset#sq(z**2-1)
def gin(z):
    return inverseoff(g,gpr,z,2j)
def gpr(z):

```

```

    return fpr(jouk(z))*(1-z**-2)

#jowkowski
def jouk(z):
    return z+1/z
def fpr(t):
    return (sq(-t**2+3))/(sq(-t**2+4))

```

Current reconstruction:

The code for our current reconstruction looks like this:

```

import numpy as np
from matplotlib import pyplot as plt
from copy import deepcopy

#Constants.
lift = .4 #lift in um
Ha = 5.1 #applied field

#following constants are only used in our brandt model
Hshielded = 1.6 #shielded field (Ha-offset)
a= 3.4+0j #part of superconductor perfectly shielded
w= 4+0j #width of superconductor

#raw data
xDatat = np.array([xDataarray])
yDatat = np.array([yDataarray])
yDatat = yDatat-Ha

#info from raw data
xrange = xDatat[-1]-xDatat[0]
xlen = len(xDatat)

#Here I extend the x-axis, and the y data.
xData = np.linspace(xDatat[0]-xrange*2,xDatat[-1]+xrange*2,num=5*len(xDatat)
)
yData = np.append(np.append(np.zeros(2*xlen), yDatat), np.zeros(2*xlen))

#greens function
def G(x):
    return x/(x**2+lift**2)

#the results seem to shift the x-axes, so I shift them back
def cutandpaste(arr):
    tele = len(arr)
    return np.append(arr[int((tele-1)/2):],arr[:int((tele-1)/2)])

#lowpass filter from chat GPT. It applies the fft to the signal and then
#sends back the filtered function in
#the fourier domain.
def lowpass_filter(signal, cutoff_frequency, sampling_rate):
    # Perform FFT on the signal
    fft_result = np.fft.fft(signal)
    # Create frequency axis

```

```

frequency_axis = np.fft.fftfreq(len(signal), d=1/sampling_rate)

# Design the custom lowpass filter in the frequency domain
filter_mask = 0.5 * (1 + np.cos(np.pi * frequency_axis /
                                cutoff_frequency))
filter_mask[np.abs(frequency_axis) >= cutoff_frequency] = 0

# Apply the filter to the signal in the frequency domain
filtered_signal_fft = fft_result * filter_mask

return np.real(filtered_signal_fft)

#brandt model function
def h(z):
    limit = np.abs((np.arctan((w)/(1j*np.sqrt(w**2-a**2)))-np.pi/2))
    temp = -Hshielded/limit*(np.arctan((w*np.sqrt(a**2-z**2))/(z*np.sqrt(w
**2-a**2)))-np.pi/2)

    if np.real(z)<0:
        return temp-np.pi*Hshielded/limit
    return temp

#create our current distribution from the brandt model (J1)
#also create our expected field By-distribution from brandt model (dist2)
J1 = deepcopy(xData)
dist2 = deepcopy(xData)
for ix,r in np.ndenumerate(xData):
    J1[ix] = np.real(h(r+.001j))
    dist2[ix] = np.imag(h(r+lift*1j))-Hshielded

#greens function
Gs = G(xData)

#Apply fft and Filter the signal yData
sampling_rate = 1000 # Hz
cutoff_frequency = 60 # Hz
filtered_signal = lowpass_filter(yData, cutoff_frequency, sampling_rate)

#fft's on G and By
by = np.fft.fft(yData, n=len(xData))
gs = np.fft.fft(Gs)

#inverse fft of the magic formula
fftandback1 = np.fft.ifft(filtered_signal/gs)

#plotting
fig, ax = plt.subplots(2)

ax[0].plot(xData,yData)
ax[0].plot(xData,dist2, color='green')
ax[0].plot(xData,np.real(np.fft.ifft(filtered_signal)), color='red')

ax[1].plot(xData,np.real(120*(cutandpaste(fftandback1)-fftandback1[200])),
           color='red')
ax[1].plot(xData,np.real(J1), color='green')

```


References

- [1] WT Norris. Calculation of hysteresis losses in hard superconductors carrying ac: isolated conductors and edges of thin sheets. Journal of Physics D: Applied Physics, 3(4):489, 1970.
- [2] EH Brandt, MV Indenbom, and A Forkl. Type-ii superconducting strip in perpendicular magnetic field. Europhysics letters, 22(9):735, 1993.
- [3] Ernst Helmut Brandt and Mikhail Indenbom. Type-ii-superconductor strip with current in a perpendicular magnetic field. Physical review B, 48(17):12893, 1993.
- [4] BRIAN D Josephson. The discovery of tunnelling supercurrents. Reviews of Modern Physics, 46(2):251, 1974.
- [5] RL Fagaly. Superconducting quantum interference device instruments and applications. Review of scientific instruments, 77(10), 2006.
- [6] Michel H Devoret, Andreas Wallraff, and John M Martinis. Superconducting qubits: A short review. arXiv preprint cond-mat/0411174, 2004.
- [7] Co Po Bean. Magnetization of hard superconductors. Physical review letters, 8(6):250, 1962.
- [8] Charles P Bean. Magnetization of high-field superconductors. Reviews of modern physics, 36(1):31, 1964.
- [9] Cun Xue, An He, Huadong Yong, and Youhe Zhou. Field-dependent critical state of high- T_c superconducting strip simultaneously exposed to transport current and perpendicular magnetic field. AIP Advances, 3(12), 2013.
- [10] Ernst Helmut Brandt. Theory of type-ii superconductors with finite london penetration depth. Physical Review B, 64(2):024505, 2001.
- [11] Kristian Fossheim and Asle Sudbø. Superconductivity: physics and applications. John Wiley & Sons, 2004.
- [12] The Editors of Encyclopaedia Britannica. "meissner effect".
- [13] Mark J Ablowitz and Athanassios S Fokas. Complex variables: introduction and applications. Cambridge University Press, 2003.
- [14] David J Griffiths. Introduction to electrodynamics. Pearson, 2013.
- [15] M. B. van Gijzen M. J. Vuik K Vuik, F.J. Vermolen. Numerical Methods for Ordinary Differential Equations. TU Delft Open, 2023.
- [16] Francesco Casola, Toeno Van Der Sar, and Amir Yacoby. Probing condensed matter physics with magnetometry based on nitrogen-vacancy centres in diamond. Nature Reviews Materials, 3(1):1–13, 2018.

- [17] Fritz London and Heinz London. The electromagnetic equations of the superconductor. Proceedings of the Royal Society of London. Series A-Mathematical and Physical Sciences, 149(866):71–88, 1935.
- [18] AV Bobyl, DV Shantsev, YM Galperin, TH Johansen, M Baziljevich, and SF Karmanenko. Relaxation of transport current distribution in a ybaco strip studied by magneto-optical imaging. Superconductor Science and Technology, 15(1):82, 2001.
- [19] JW Zuber, Frederick S Wells, Sergey A Fedoseev, Tom H Johansen, Anatoly B Rosenfeld, and Alexey V Pan. A new approach to the inverse problem for current mapping in thin-film superconductors. Journal of Applied Physics, 123(12), 2018.
- [20] Bradley J Roth, Nestor G Sepulveda, and John P Wikswo Jr. Using a magnetometer to image a two-dimensional current distribution. Journal of applied physics, 65(1):361–372, 1989.
- [21] A.V. Oppenheim, A.S. Willsky, and I.T. Young. Signals and Systems. Prentice-Hall signal processing series. Prentice-Hall, 1983.